Phys. Rev. C 91 (2015) 024310 **LA-UR-14-24999**

Fission barriers at the end of the chart of the nuclides

Peter Möller,[1,*] Arnold J. Sierk,[1] Takatoshi Ichikawa,[2] Akira Iwamoto,[3] and Matthew Mumpower[4]

[1] *Theoretical Division, Los Alamos National Laboratory, Los Alamos, New Mexico 87545, USA*
[2] *Yukawa Institute for Theoretical Physics, Kyoto University, Kyoto 606-8502, Japan*
[3] *Advanced Science Research Center, Japan Atomic Energy Agency (JAEA), Tokai-mura, Naka-gun, Ibaraki, 319-1195, Japan*
[4] *Joint Institute for Nuclear Astrophysics, University of Notre Dame, 225 Nieuwland Science Hall, Notre Dame, IN 46556, USA*

(Dated: August 25, 2015)

We present calculated fission-barrier heights for 5239 nuclides, for all nuclei between the proton and neutron drip lines with $171 \leq A \leq 330$. The barriers are calculated in the macroscopic-microscopic finite-range liquid-drop model (FRLDM) with a 2002 set of macroscopic-model parameters. The saddle-point energies are determined from potential-energy surfaces based on more than five million different shapes, defined by five deformation parameters in the three-quadratic-surface shape parameterization: elongation, neck diameter, left-fragment spheroidal deformation, right-fragment spheroidal deformation, and nascent-fragment mass asymmetry. The energy of the ground state is determined by calculating the lowest-energy configuration in both the Nilsson perturbed-spheroid (ϵ) and in the spherical-harmonic (β) parameterizations, including axially asymmetric deformations. The lower of the two results (correcting for zero-point motion) is defined as the ground-state energy. The effect of axial asymmetry on the inner barrier peak is calculated in the (ϵ, γ) parameterization. We have earlier benchmarked our calculated barrier heights to experimentally extracted barrier parameters and found average agreement to about one MeV for known data across the nuclear chart. Here we do additional benchmarks and investigate the qualitative, and when possible, quantitative agreement and/or consistency with data on β-delayed fission, isotope generation along prompt-neutron-capture chains in nuclear-weapons tests, and superheavy-element stability. These studies all indicate that the model is realistic at considerable distances in Z and N from the region of nuclei where its parameters were determined.

PACS numbers: 24.75.+i,25.85.Ec,26.30.Hj,21.60.n

I. INTRODUCTION

In actinide fission a nucleus typically evolves from a single nucleus in its deformed ground state to two separated fragments: one large roughly spherical fragment with nucleon number $A \approx 140$ and a smaller deformed fragment with the remainder of the nucleons. In Ref. [1] we presented calculations of fission potential-energy surfaces and associated barrier heights for 1585 nuclei, and some conclusions based on these studies. We now extend the study and tabulate barriers for 5239 nuclides in the region $171 \leq A \leq 330$ for all nuclei between the proton and neutron drip lines. All aspects of the calculations are identical to those presented in Ref. [1] where full details are given. However, we review both some important ingredients and features of our approach and how it is positioned with respect to other fission-barrier calculations. An overview of the results is presented in Figs. 1 and 2.

We have previously made the case that to study the nuclear potential energy during the shape evolution in fission and to allow the nucleus freedom to evolve into fragments with different shapes and into different fragment mass divisions, it is necessary to calculate the nuclear potential energy as a function of, at a minimum, five shape degrees of freedom corresponding to: elongation, neck radius, left fragment shape, right fragment shape and the asymmetry of the mass division [1, 3–6]. It is also necessary to space the deformation points fairly densely so that shell-structure features appear accurately in the calculated potential-energy surfaces. As an example, consider the shell-structure effects in the tin-like fragment with $A \approx 140$. In ground-state mass calculations in which the associated microscopic corrections are also tabulated, for example in the FRDM(1992) mass calculation [7] we find that the ground-state microscopic corrections for ${}^{132}_{50}\mathrm{Sn}_{82}$, ${}^{130}_{50}\mathrm{Sn}_{80}$, and ${}^{130}_{48}\mathrm{Cd}_{82}$ are -11.55 MeV, -9.14 MeV, and -9.85 MeV, respectively. Thus, near magic numbers a change by one nucleon changes the microscopic correction by about 1 MeV. See Ref. [7] for precise definitions of the shell-plus-pairing correction, and the associated microscopic correction. The latter quantity is a sum of the shell-plus-pairing correction, the deformation change of the macroscopic energy relative to the sphere and a zero-point energy. We therefore space our asymmetry coordinate so that one step in the asymmetry coordinate corresponds to moving about one proton and one neutron from one fragment to the other. For example, for an $A = 200$ nucleus the symmetric configuration obviously corresponds to a mass division $M_{\mathrm{H}}/M_{\mathrm{L}} = 100/100$ and our next grid point in the asymmetry coordinate corresponds to $M_{\mathrm{H}}/M_{\mathrm{L}} = 102/98$ where M_{H} is the heavy-

* moller@lanl.gov

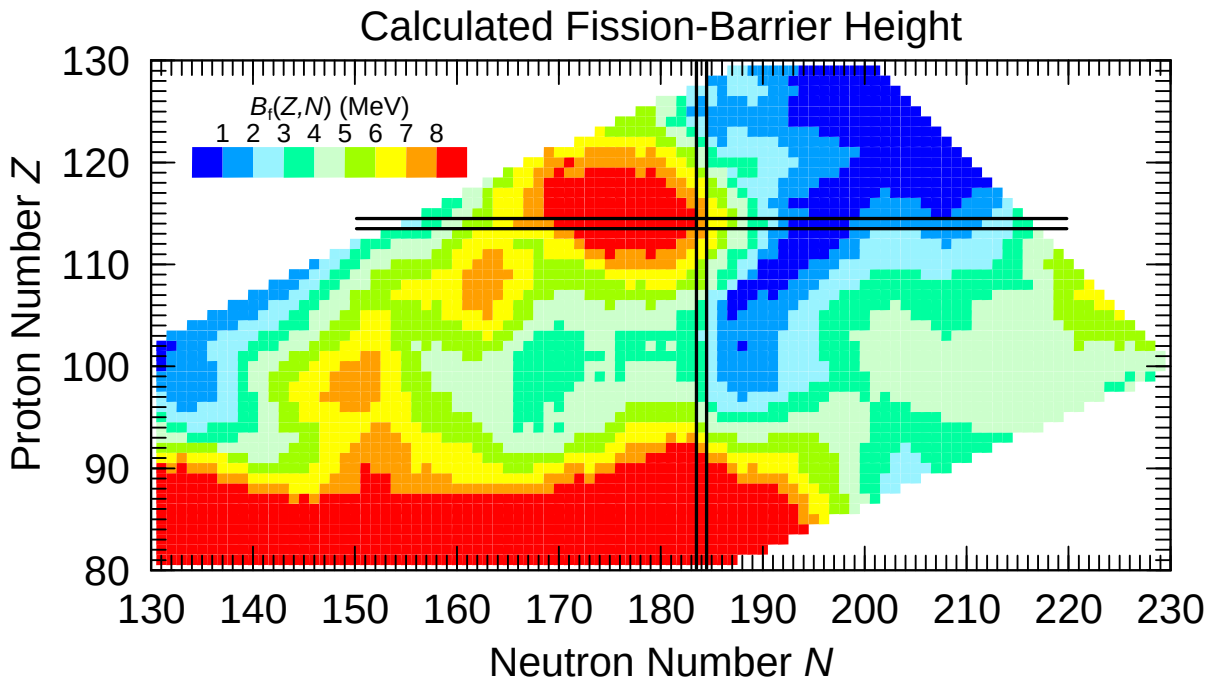

FIG. 1. (Color online) Calculated fission-barrier heights for 3282 nuclei. The highly variable structure is mostly due to ground-state shell effects. Ground-state shell effects are particularly strong in the deformed regions around $^{252}_{100}\mathrm{Fm}_{152}$ and $^{270}_{108}\mathrm{Hs}_{162}$ and in the nearly spherical region near the next doubly-magic nuclide postulated to be at $^{298}_{114}\mathrm{Fl}_{184}$. Our strongest shell effects are slightly offset to the left with respect to this isotope.

fragment mass and M_L is the light-fragment mass. To allow studies of cold-fusion heavy-ion reactions on $^{208}_{82}\mathrm{Pb}_{126}$ targets leading to superheavy elements, we use 35 grid points in the asymmetry coordinate [1]. In the elongation coordinate Q_2 we use 45 grid points; in the remaining three deformation coordinates, 15 in each. This leads to more than 5 000 000 shapes. It should be obvious, but is perhaps not immediately intuitively clear that the consequence is large data storage needs. If the energies for each shape for each of the about 5000 nuclei is stored as a 10 digit number this means that the total data storage space needed is $5\,000\,000 \times 10 \times 5\,000 = 2.5 \times 10^{11}$ bytes, that is 250 Gb of storage. When we started this type of calculation based on millions of shapes in 1999, [3], this was indeed a problem; now it is not.

II. OTHER FISSION POTENTIAL-ENERGY CALCULATIONS

In most previous fission studies various schemes were employed to avoid calculating a complete "hypercube" in all the deformation variables considered. Such complete calculations were impractical until computer performance had evolved sufficiently, roughly achieved around 1995–2000. In macroscopic-microscopic calculations it was the norm to plot energies versus two shape variables, for example β_2 and β_3 (quadrupole and octupole deformations) and "minimize" the potential energy with respect to additional multipoles; typical examples are Refs. [8, 9]. Although such approaches intuitively seem promising, there are significant concerns about the uniqueness and stability of such results. First, when minimizations are carried out at a specific location (β_2, β_3), what are the starting values of the additional shape variables over which the minimization is carried out? A trivial suggestion is that the values obtained for a previous point be used, but which is the "previous point" will depend upon the sequence in which the grid points are considered. It is easy to visualize a surface, even in two dimensions, for which a different result may be found by approaching a particular point from opposite directions. Another strategy could be that the minimizations are started at the value zero of the additional variables at each point (β_2, β_3), but these approaches would miss possible multiple deformed minima. And, even if found, it would be impossible to display multiple minima versus the "hidden" shape variables in a two-dimensional contour plot. Furthermore, none of these methods, which only access a limited part of the higher dimensional space, are guaranteed to find the true saddle points with reasonable accuracy. In some cases, the saddle solutions will be correct, but there is no way to mathematically evaluate the possible errors inside the model framework itself. In many of these minimization studies points that seem near each other in the two-dimensional (β_2, β_3) plots are actually

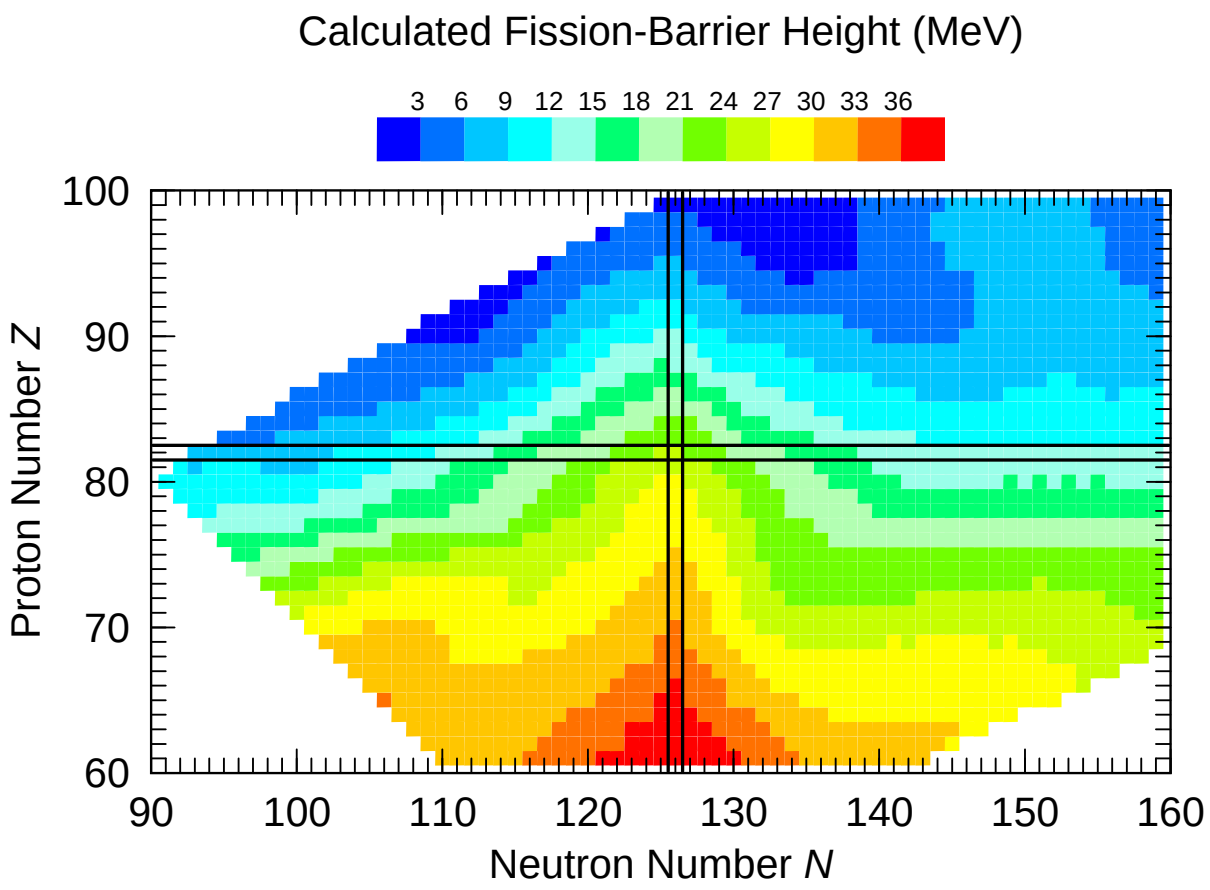

FIG. 2. (Color online) Calculated fission-barrier heights for 2113 nuclei with generally lower proton and neutron numbers than those in Fig. 1. Because the macroscopic energy contributes the major part of the fission-barrier height for most nuclei in this region, and because of the different energy scale compared to Fig. 1, the only shell effects clearly visible come from the $N = 126$ spherical neutron shell.

quite distant in the higher-dimensional space. This is often manifested as strong discontinuities appearing in published potential-energy contour diagrams or plots of energy surfaces. Despite these known deficiencies, these methods are still in routine use today [10]. However, very recently other groups previously employing such approximations have come to the conclusion that the minimization method is deficient, not just in principle but also in practice. In one recent macroscopic-microscopic model study, the calculations were carried out for complete multidimensional "hypercubes" and confirmed that the immersion methods we employ are crucial to avoiding spurious results from the use of minimization. It is stated directly *"This shows that the minimization is an uncertain method of the search for saddles . . . "* in the summary conclusions [11]. This study also directly contradicts large axial asymmetry effects found at fission saddle points with essentially the same macroscopic-microscopic model by use of minimization in Ref. [10].

Currently, the main alternative approach to macroscopic-microscopic calculations of fission-barrier potential-energy surfaces and saddle points is the constrained Hartree-Fock method introduced in 1973 [12]. Those authors state *"One of the advantages of this type of calculation is that deformation energy curves can be calculated without making a complete map of the deformation energy surface"*. Another comment that is often made in connection with determining fission saddle points is that "constrained selfconsistent methods automatically take all higher shape degrees of freedom into account". However, these statements are misleading. Imposing shape constraints in selfconsistent methods is mathematically equivalent to the use of minimization techniques in macroscopic-microscopic methods, which we, and now other groups, have demonstrated are flawed. A detailed discussion is in Ref. [1]. A very transparent discussion coming from outside the field of nuclear physics is in Ref. [13]. The example used there is the determination of the Continental Divide in the United States, but the problem is essentially identical to that of finding saddle points in potential-energy surfaces, although easier to visualize because geographical

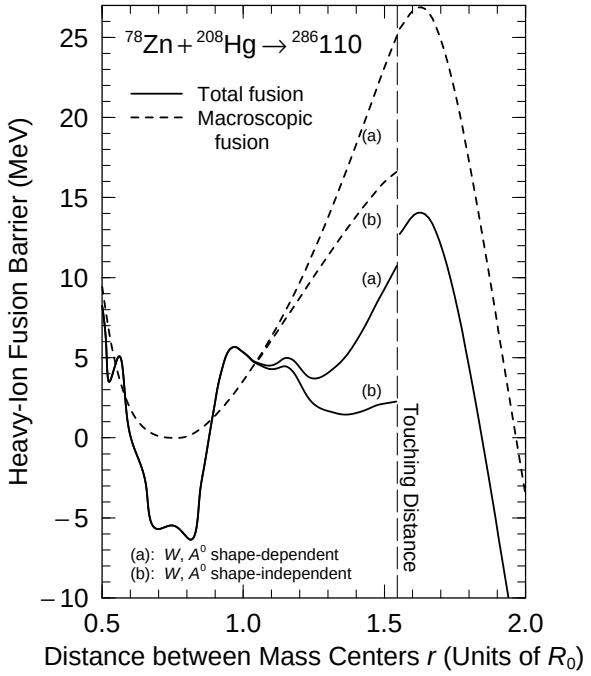

FIG. 3. Calculated macroscopic and total potential energies, for shape sequences leading to the touching configuration, at the long-dashed line, of spherical ^{78}Zn and ^{208}Hg. To the left the calculations trace the energy for a *single, joined* shape configuration, from oblate shapes through the spherical shape at $r = 0.75$ to the touching configuration at $r = 1.52$; to the right the calculations give the energy for separated spherical nuclei beyond the touching point. The continuous path through five-dimensional space from the ground state to the touching configuration is arbitrary; the key point is that the limiting shapes when approaching the line of touching from the left and right are identical, namely spherical ^{78}Zn and ^{208}Hg in contact. At a specific value of r all curves are calculated for the same shape. To obtain continuity of the macroscopic energy at touching, a crucial feature in realistic models, it is essential that various model terms depend appropriately on nuclear shape, as is the case for the curves (a). The slight remaining discontinuity in the *total* fusion energy curve (solid line) arises because the Fermi surfaces of the nuclei readjust at contact, and because pairing and spin-orbit strength parameters also undergo small discontinuous changes there. This figure and caption are adapted from Ref. [2]

topography is studied in 2D spaces only.

It has been suggested that when constrained HF or HFB calculations are presented, for example as two-dimensional contour maps a *necessary* condition to impose on the results is that the spatial overlap between the wave-functions for neighboring grid points in the contour plot should be large. If there exist neighbor points that do not fulfill a required overlap criterion, then one would need to go from 2 to 3 constraints, or in the general case add one additional constraint and again impose the continuity check [14]. But even if the potential energy obtained with two constraints corresponds to a continuous variation of the densities, it is by no means certain a saddle point on this surface is a good approximation to the real (lowest) saddle point, see for example the discussion of figure 5 in Ref. [1]. Based on these observations of problems with existing alternative methods and the evidence from our multitude of benchmarks, see below, we feel that the approach we use is the most accurate currently available for large-scale calculations of databases of various fission-barrier properties.

III. SUMMARY OF ESSENTIAL MODEL FEATURES

In the macroscopic-microscopic model the energy for a specific, prescribed nuclear shape is calculated as a sum of a macroscopic energy and a microscopic shell-plus pairing correction. In the community, several different models are used for the macroscopic and the microscopic parts. For example, the microscopic part can be based on a modified-oscillator (Nilsson) single-particle potential [15, 16], a Woods-Saxon single-particle potential [17], a folded-Yukawa single-particle potential [18], and others. We use what we have called the finite-range liquid-drop model (FRLDM) [19] for the macroscopic part and the folded-Yukawa single-particle model as the starting point for the microscopic part. When we refer to the full macroscopic-microscopic model, we for brevity use the notation FRLDM when the macroscopic part is the finite-range liquid-drop model and FRDM when the macroscopic part is based on the finite-range droplet model; we do not use the latter in our fission-barrier calculations, for reasons we explain below.

A. Macroscopic model

For the macroscopic energy we use the finite-range liquid-drop model (FRLDM). Briefly stated, it is based on a standard shape-dependent "liquid-drop" model [20, 21], which is enhanced to take the finite range of the nuclear force [19] and the diffuseness of the charge distribution [22] into account. In the original liquid-drop model, the surface energy is strictly proportional to the surface area of the nucleus [23]. For shapes with well-developed small-radius necks, this leads to too high a surface-energy contribution to the macroscopic energy in the neck region. For such shapes the finite range of the attractive nuclear force may be thought of as reaching across the neck region to nucleons on the opposite side of the neck, leading to a reduction of the surface energy. The effect is also important in calculations of heavy-ion interaction barriers and even for some ground-state shapes containing higher-multipole components. An in-depth presentation of the model and discussions of these issues are found in Refs. [7, 19, 22].

When fission was discovered [24], it was realized that the observations could be interpreted in terms of a macroscopic, deformable liquid-drop model [25, 26]. Bohr and

Wheeler very soon afterward presented a quantitative description of the shape dependence of the surface and Coulomb energies in terms of Taylor expansions and obtained the systematics of fission-barrier heights for nuclei throughout the periodic system [23].

To model nuclear masses more accurately than was possible with the original liquid-drop model, or semi-empirical mass model [27], phenomenological shell corrections with adjustable parameters were often added to the macroscopic expression. In these studies it was observed that in addition to a strong contribution from microscopic effects at and near magic numbers, it was necessary to account for the extra binding that was observed for nuclei with equal or nearly equal proton and neutron numbers [20]. One commonly used form for this "Wigner energy", which we use, is

$$E_{\rm W} = W \left[\frac{|N-Z|}{N+Z} \right], \qquad (1)$$

where for the Wigner constant W, we use the value 30 MeV. In nuclear mass models this term was customarily included without a shape dependence. For a ^{236}U nucleus this contribution to the nuclear potential energy is 6.6 MeV. However, if we use the model to describe the highly-deformed shapes in fission near the transition from a single shape to two fragments, it is relevant to ask if this shape-independent formulation makes sense. For example, for the simple case of two touching spheres we would hope to get the same calculated energy if we consider the system as one very deformed single shape, or as two separate touching nuclei. Clearly, if we consider any division of the original nuclear system with proton and neutron numbers $Z_{\rm comp}$ and $N_{\rm comp}$ into two fragments (1) and (2) with proton and neutron numbers Z_1, N_1, Z_2, and N_2 while preserving neutron–proton asymmetry, that is

$$Z_1 = \alpha \times Z_{\rm comp} \quad N_1 = \alpha \times N_{\rm comp}$$

and

$$Z_2 = (1-\alpha) \times Z_{\rm comp} \quad N_2 = (1-\alpha) \times N_{\rm comp}$$

where α is a fractional number in the range 0–1, then there will be a Wigner energy contribution $E_{\rm W} = 6.6$ MeV to each of the touching nuclei. Thus for the touching configuration there will be a difference 6.6 MeV in calculated potential energy if it is treated as a scission configuration or as two touching nuclei. Obviously, for the touching configuration one would also need to take into account the interaction energies between the two nuclei. After doing this, to avoid this 6.6 MeV remaining discontinuity, it is necessary to introduce a shape dependence for the Wigner energy, so that

$$E_{\rm W} = W \left[\frac{|N-Z|}{N+Z} \right] B_{\rm W}, \qquad (2)$$

where the shape-dependent function $B_{\rm W}$ evolves continuously from $B_{\rm W} = 1$ for a shape with no discernible neck to $B_{\rm W} = 2$ as the shape evolves into separated fragments. These issues are further discussed in [28] where the exact expression we use for the deformation dependence of $B_{\rm W}$ is given. The specific functional form for this dependence is not derived, but is arbitrarily defined to smoothly transition from a value of 1 to a value of 2 as a function of the developing neck. Similar considerations show that it is necessary to introduce a shape dependence for the constant, "$a_o A^0$ term", that occurs in the FRLDM. The FRLDM used in our calculations is completely specified in [7] in section 3.5, except that the above shape dependencies were not introduced. Thus the constant and Wigner terms in Eq. (62) in [7] are generalized to

$$\begin{aligned} &E_{\rm macr}(Z,N,\text{shape}) = \ldots \\ &+ a_0 A^0 B_{\rm W} \\ &+ W \left(|I| B_{\rm W} + \begin{cases} 1/A & , \ Z \text{ and } N \text{ odd and equal} \\ 0 & , \ \text{otherwise} \end{cases} \right) \\ &\ldots \end{aligned} \qquad (3)$$

Potential-energy calculations without and with these shape-dependencies are shown in Fig. 3. The slight discontinuity in the "Total fusion" curve is mainly due to the equalization of the Fermi surfaces of the two colliding nuclei that occurs after contact.

Because, in our studies since the year 1999, we have calculated fission potential-energy surfaces for several million deformation-grid points, this has systematically lowered all calculated fission saddle-point energies compared to those calculated previously using a much smaller space of shapes. The macroscopic-model constants thus had to be readjusted by a simultaneous fit to experimental barrier heights and ground-state masses, leading to different macroscopic parameters from those in [7], referred to as FRLDM(1992). We now use the constants FRLDM(2002), given in Ref. [2].

We emphasize that in nuclear mass calculations we obtain the most accurate results by use of the finite-range droplet model (FRDM). This model is a combination of the FRLDM and the droplet model [29], which allows, at a macroscopic level, calculation of effects of Coulomb redistribution (some charge is pushed from the center toward the surface) and other related effects. These effects lead to about a 15% improvement in mass-model accuracy. But the droplet model enhancement introduces many terms that are derived as expansions in terms of small deformations around a spherical shape. It is therefore not possible to take it to large deformations and make a continuous energy transition at scission to separated shapes using this macroscopic model. Therefore it can not be used in calculations of fission potential-energy surfaces. In our study of masses in Ref. [7] we actually performed a limited calculation of fission-barrier heights in the FRDM and the model parameters were determined by adjusting to a weighted sum of masses and barrier heights. At that time the barrier saddle points were

determined from a 1973 calculation [30, 31] in a three-dimensional space containing only 175 different shapes. The saddle shapes obtained in this calculation did not exhibit obvious neck indentations (and as we now realize were not very realistic [3, 4]) so we did not address the issue that the droplet model and the FRDM become increasingly inaccurate at large deformations. This is why we now in fission calculations use only the FRLDM.

B. Microscopic model

The shell-plus-pairing corrections are calculated by use of Strutinsky's method from single-particle levels in a folded-Yukawa potential. The single-particle potential is almost unchanged since 1973 [18, 32], except that in 1980, to permit application to the whole nuclear chart, we let the neutron and proton spin-orbit strengths depend weakly on the nucleon number A [33]. The shell-plus-pairing corrections are calculated as described in [18] with the following enhancements. First, to avoid the well-known collapses of the BCS method, we now use a Lipkin-Nogami pairing model implemented as explained in detail in [34]. Again, imposing continuity at scission required that some constants of the Strutinsky and pairing models depend on deformation, which is discussed in detail in [7, 28]. Full details of the current implementation of the microscopic model are given in Ref. [7], including values of all its constants and various shape dependencies, if any.

C. Deformation grid

Although many of the essential features of the macroscopic-microscopic model were developed up to 40 years ago, it is the continuous increase in computer power that has made it possible to exploit its full potential. In calculations 40 years ago, theoretical studies of mass asymmetry in fission had to be based on potential-energy surfaces calculated for only for a very few shapes: for example versus two independent deformation coordinates for 20 shapes in an early (1970) study [35] versus 3 independent shape coordinates for 175 shapes in 1973 [30]. The 1973 calculation took about 30 hours on a CDC 6600, at Los Alamos Scientific Laboratory, a computer shared by hundreds of researchers. Both these (and other) calculations obtained mass-asymmetric outer saddle points but beyond the outer saddles the potential-energy contour plots developed the deepest "valley" for shapes corresponding to symmetric divisions, in apparent contradiction to experimentally observed asymmetric fragment splits. These results were dismissed by comments like "valleys are not invariant under coordinate transformation" [30] (an observation originally emphasized by Wilets [36]) or, that dynamics determined the final outcome. However, the asymmetry in actinide fission was almost since its discovery explained in a hand-waving fashion as due to a preference of the system to divide into one fragment as close as possible to the spherical, doubly-magic ^{132}Sn nucleus and a remainder, a smaller, deformed fragment. Thus, to permit the potential energy to contain all deformation features related to such divisions one needs to calculate the potential, as stated previously, versus at least five shape degrees of freedom: elongation, neck radius, the two nascent-fragment shapes, and mass asymmetry. In the three-quadratic-surface parameterization one can by suitable manipulations of the expressions involved, see Ref. [1], use these variables, which have an obvious intuitive interpretation, to specify the deformation grid. Also, in this grid the five different shape coordinates are, loosely speaking, nearly orthogonal, which permits a quick, intuitive interpretation of the calculated 5-dimensional potential-energy surfaces. Recently we have also shown that calculations of fission-fragment yields based on a simple "random walk" in this 5D space and the Metropolis algorithm gives excellent agreement with experimental data [37–39]. This suggests two conclusions. First, the coordinate choice and spacing is quite consistent with intuitive interpretations; otherwise it would not have been possible to interpret in a straightforward fashion the features of the potential-energy surface in terms of symmetric and asymmetric valleys, different saddle points leading into these different valleys, and ridges in between [1, 6], nor would the Metropolis algorithm have given as realistic results as it now does. Second, we can conclude, because the yield calculations reproduce the substantial differences between the ^{236}U and ^{240}Pu yields [37] that the calculated potential energy is realistic also beyond the outer saddle points, which had not been clearly established earlier, although some hints had been seen in calculations of the most-probable mass divisions [6]. The algebra that is involved in taking the above intuitive coordinate concepts into the actual expressions that in the three-quadratic-surface parameterization generate these shapes is rather tedious and we therefore direct the reader to Ref. [1] for details.

Axially asymmetric deformations are also investigated, but these studies are limited to the ground state and the inner-barrier saddle point. Since the three-quadratic-surface shapes are not able to generate optimal ground-state shapes for some nuclei we have furthermore calculated ground-state energies in the ϵ and β parameterizations. Again, the precise definitions of the deformation grids in these three additional potential-energy calculations are given in Ref. [1], where also details on how the barrier heights are extracted based on the combined information contained in these four complementary potential-energy surfaces are given.

IV. RESULTS

We have calculated barrier heights $B_{\rm f}$ for 5239 nuclides exactly as described in Ref. [1] and references cited

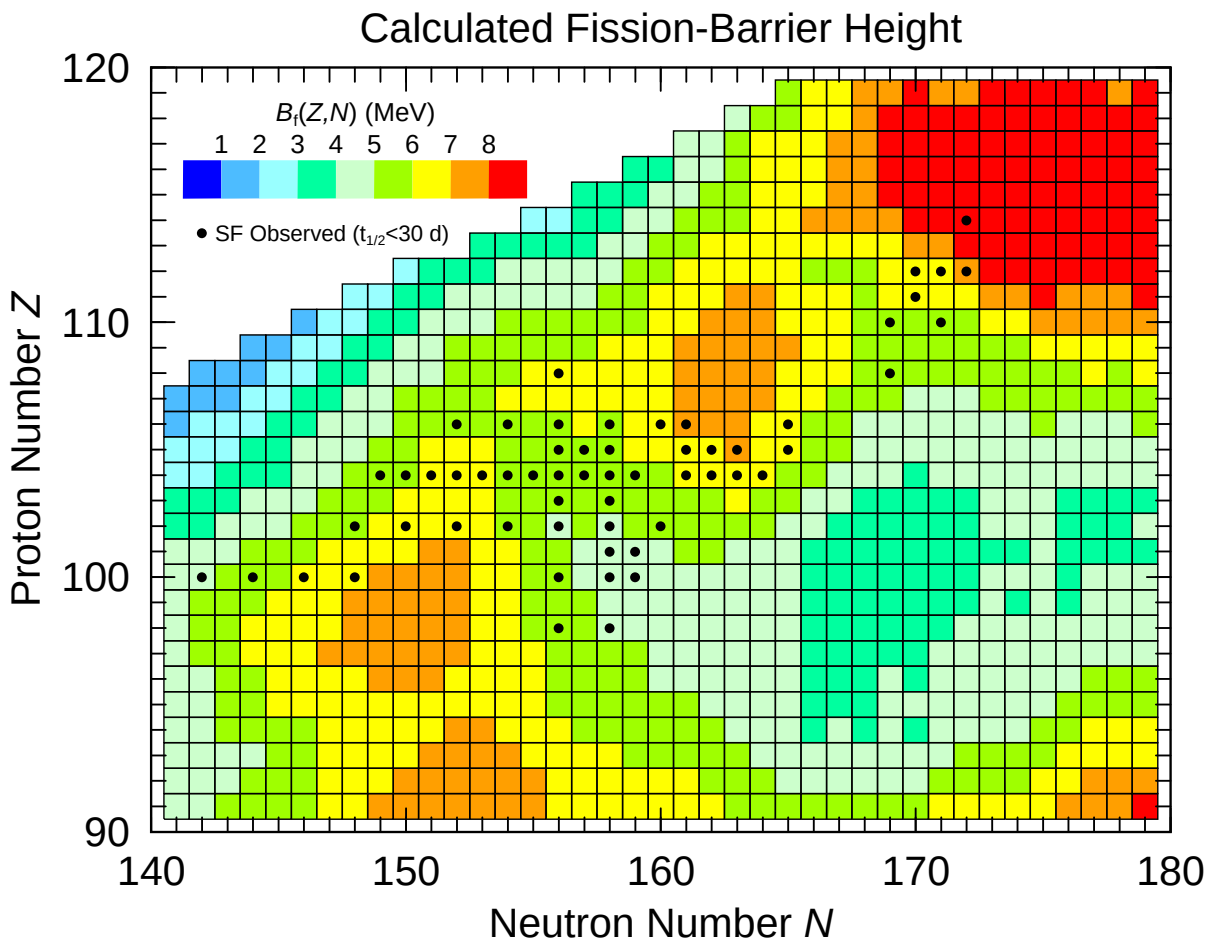

FIG. 4. (Color online) A more detailed look at fission-barrier heights for 980 nuclei in the heaviest region. We have marked with black dots those nuclides for which spontaneous fission with a half-life under about 30 days has been observed.

therein. We have summarized the model features in the section above, in particular facts and features that might be somewhat time consuming to trace in a quick scan of the references. The barriers are tabulated in Table I.

The fission-barrier properties of our model have previously been benchmarked with respect to known data for nuclides near β-stability. We have shown that we reproduce the outer barrier peak height for 31 nuclides from $^{70}_{34}\mathrm{Se}_{36}$ to $^{252}_{98}\mathrm{Cf}_{154}$ with an rms deviation of only 1.0 MeV [2]. We have also compared calculated actinide inner and outer barrier heights as well as the height of the fission-isomer minimum to barrier parameters extracted from various types of experimental data, often cross sections as functions of energy for neutron-induced fission [1]. In this context we observe that the "experimental" barrier parameters are not as directly measured data as, for example, nuclear masses are in some experiments. The "experimental" barrier parameters are numbers occurring in models of experimental cross sections. Moreover, these models almost always assume one-dimensional barriers whereas our barrier parameters refer to saddles and minima in five-dimensional deformation spaces. Further complicating the situation is that different evaluations (of different sets of experimental data, and/or just using different cross-section models) often lead to different results for the extracted barrier parameters. For example Blons and collaborators [40] consistently find that the so called "third minima" of some light actinide nuclei are very shallow and no more than 0.5 MeV or so below the surrounding second and third barrier peaks, which are about 6 MeV above the ground-state minimum, in good agreement with results obtained in our current model [41]. In contrast, Csige and collaborators [42–44] find third minima for nuclei in this region that are up to 3 MeV below the surrounding peaks. We find it difficult to reconcile with potential-energy calculations the substantial difference in barrier structure they find between $^{232}_{92}\mathrm{U}_{140}$ [42] and $^{232}_{91}\mathrm{Pa}_{141}$ [43] in these studies. A change by just one proton and one neutron cannot, in potential-energy calculations, result in such large differences in barrier structure. For these reasons we refer to Figs. 23–32 in Ref. [1] for a qualitative benchmark of our

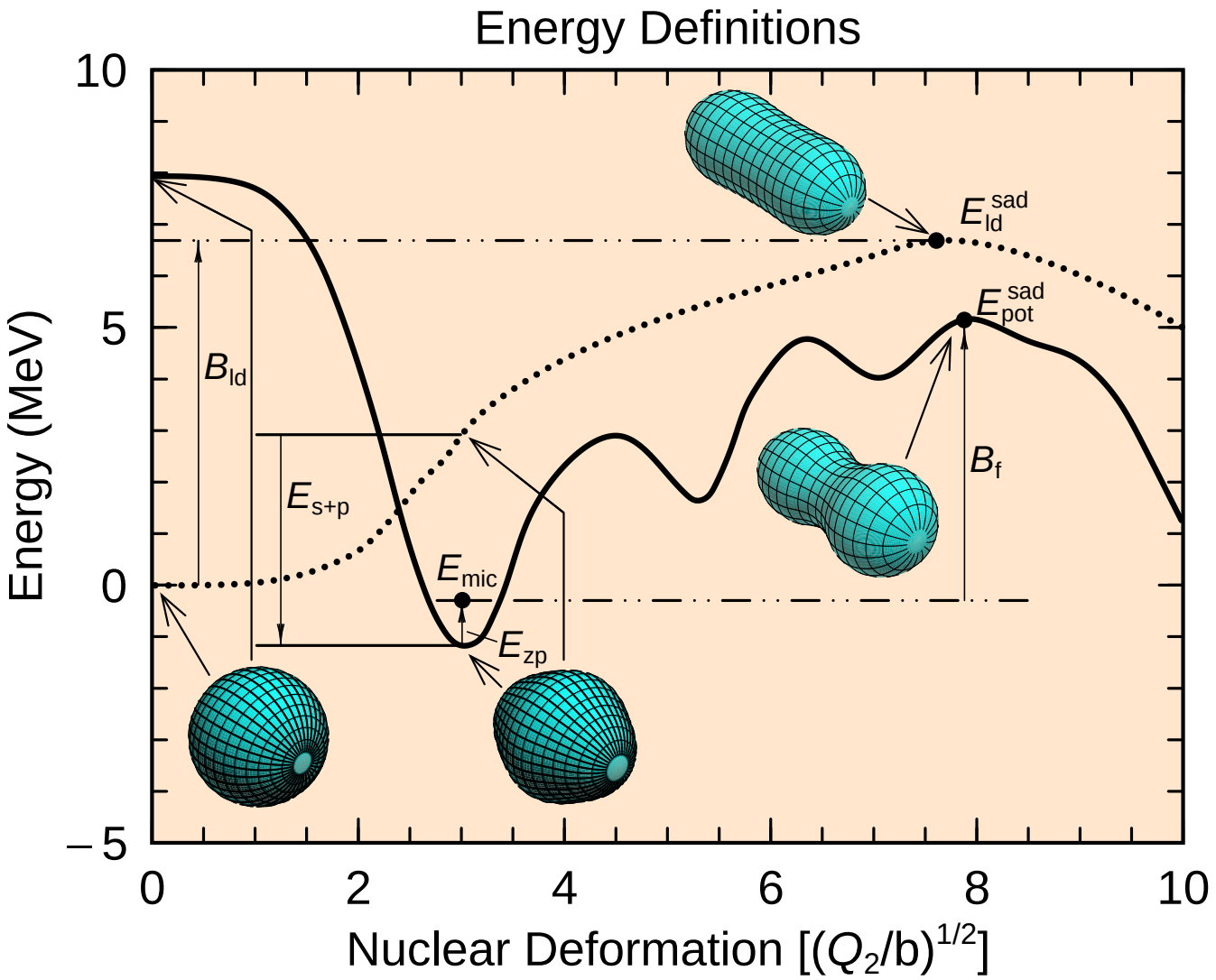

FIG. 5. (Color online) Various energy concepts used in macroscopic-microscopic fission potential-energy calculations. The dotted line is the macroscopic "liquid-drop" energy along a specified path; the solid line is the total macroscopic-microscopic energy along a partially different shape sequence. So that the various energy concepts can be illustrated, the shapes for which the energies have been calculated are: At $Q_2 = 0$ the energies are calculated for a spherical shape. For the shapes from the sphere to the ground-state shape, the shapes are the same for both curves and chosen so that they evolve continuously from the sphere to the calculated macroscopic-microscopic ground-state shape. From the ground state towards larger deformations the total-energy curve is along the optimal fission path that includes all minima and saddle points identified along this path in the five-dimensional deformation space; the liquid-drop-energy curve joins smoothly the macroscopic energy for the shape at the macroscopic-microscopic ground-state (which is not the lowest macroscopic energy at this value of Q_2) to the liquid-drop-model saddle point. The energies are calculated for ^{232}Th. Some important shapes are also shown.

calculations with respect to barrier parameters derived from analysis of experimental cross sections, rather than relying on a calculation of an rms deviation between our model calculations and model-dependent "experimental" barrier parameters with inherently similar levels of uncertainty. Such quantitative indicators are easy to misuse for a spurious sense of precision.

Barrier heights have also been estimated from electron-capture (EC) delayed fission data; for some recent discussions see [1, 45, 46]. In EC-delayed fission, daughter states up to the electron-capture Q-value $Q_{\rm EC}$ are populated. However phase-space properties result in daughter population probabilities that are roughly proportional to $(Q_{\rm EC} - E^*)^5$ where E^* is the excitation energy above the ground state in the daughter. Therefore the decay intensities to sufficiently high energies so that EC-delayed fission occurs are usually low. For EC-delayed fission to be observable a rough rule of thumb is that

$$Q_{\rm EC} \gtrapprox B_{\rm f} - 2 \ \text{MeV} \qquad (4)$$

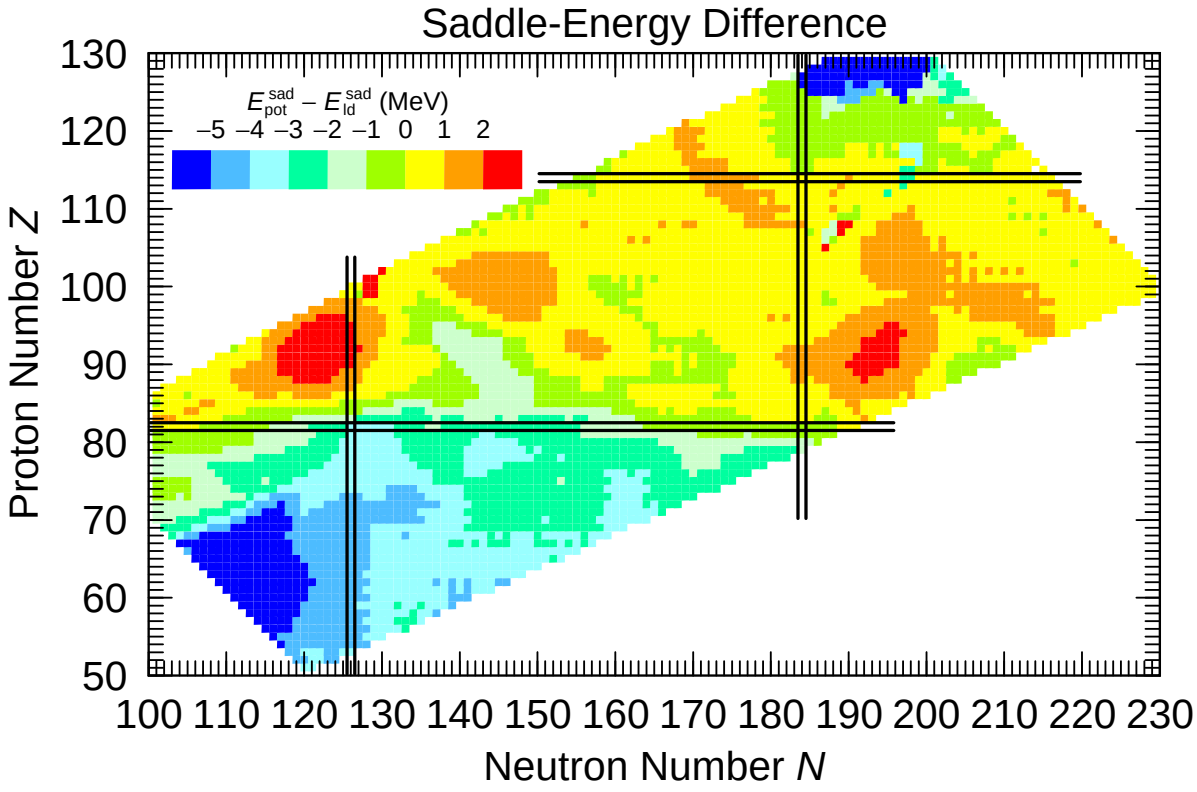

FIG. 6. (Color online) Difference between the saddle-point energy obtained from the five-dimensional macroscopic-microscopic potential-energy surface and the saddle-point energy obtained from a surface in the same deformation space using only the macroscopic model for 5139 nuclei.

We show in Fig. 34 and Table V in Ref. [1] the degree to which our calculated masses and fission-barrier heights satisfy this empirical "rule." With the possible exceptions of a couple of nuclei near $N = 150$, all the observed cases of EC-delayed fission are consistent with our model values. As discussed in Ref. [1], this exception probably occurs because the calculated $N = 150$ neutron gap in the single-particle spectrum in our model is somewhat too large, resulting in too low ground-state energies and slightly too high barriers. But in general the relation is well fulfilled in this comparison, which tests the model far from stability, towards the proton-rich side, across the wide region $80 \leq Z \leq 99$ and $100 \leq N \leq 150$.

Calculated barrier heights for 3282 nuclides in the heaviest region are plotted in Fig. 1. Above $Z \approx 100$ the macroscopic contribution to the fission barrier is very low. Therefore survival with respect to spontaneous fission (SF) and the high barriers that are the reason for the long SF half-lives are mainly due to negative ground-state microscopic corrections [47, 48], which can be substantial in some localized regions. We observe such localized regions of high fission barriers in the vicinity of $^{252}_{100}\mathrm{Fm}_{152}$, $^{270}_{108}\mathrm{Hs}_{162}$, and in the superheavy-element (SHE) region. In our calculations the maximum ground-state microscopic correction occurs at $Z = 116$ and $N = 178$, rather than at $Z = 114$ and $N = 184$ [7]. The regions of high fission barriers coincide with regions of large ground-state microscopic corrections which can exceed (in the negative direction) -6 MeV also for deformed nuclei outside the spherical superheavy region near $Z = 114$ and $N = 184$, namely in the deformed regions centered at $^{252}_{100}\mathrm{Fm}_{152}$ and $^{270}_{108}\mathrm{Hs}_{162}$. Along the Fm isotope chain the barrier heights decrease rapidly with distance from $N = 152$, and the spontaneous fission half-lives show a similar rapid decrease, which is reproduced in numerous calculations, for example Refs. [28, 49–53].

In Fig. 2 we display calculated barriers for 2113 nuclei for the lighter region in our study. There is less structure here compared to the heavier region in Fig. 1. In this region, the macroscopic energy contributes significantly to the barrier height, leading to the use of a different energy scale in this figure. Therefore, the only easily discernible shell structure is due to the magic neutron number $N = 126$.

For a long time $Z = 99$ as been the upper limit for reasonably accurate experimental fission-barrier parameters [54–57]. Only recently has a barrier height for a heavier system, ^{274}Hs, been determined [58]. However, spontaneous fission has been observed for many heavier systems. We can use these data to further benchmark

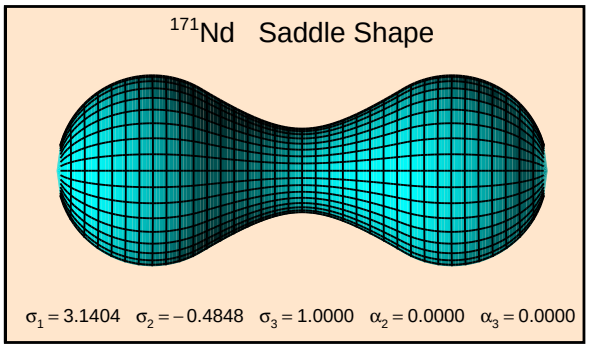

FIG. 7. (Color online) Shape of $^{171}_{60}\mathrm{Nd}_{111}$ at the saddle point.

our calculated barrier heights. In Fig. 4 we show in more detail a limited set of the data in Fig. 1, namely nuclei from the actinide region up to $Z = 120$. We show as black dots those nuclei for which spontaneous fission has been observed with a half-life less than 30 days, taken from the compilation of Ref. [59]. The aim is to investigate what correlations we find between the calculated barrier heights and the observed fissioning nuclei. This is only to get an overview of the situation because we do not

- show that most nuclei in this plot have not been observed experimentally.
- account for the highly variable effect of specialization energies in odd-even and odd-odd nuclei on spontaneous fission half-lives; this effect can increase half-lives by a factor 10^1 to a factor 10^9 [49].
- account for the branching ratios between α-decay and fission. For example a system may have a spontaneous fission half-life of, say, one second, but SF may still not be observed because the α-decay half-life is in the microsecond range.

Despite these limitations we see some interesting correlations that support the accuracy of the calculated barriers. SF is almost exclusively observed in the regions where the predicted barrier is between slightly below 5 MeV and 7 MeV, with only 4 exceptions out of 58 data points. So we conclude from these qualitative arguments that our barrier heights are consistent with the observed occurrences of SF in the heavy-element region.

In some calculations of fission barriers, it is assumed that the shell-plus-pairing corrections at the saddle are small and can be neglected, whereas the shell-plus-pairing corrections at the ground states always have to be included. Refs. [47, 48, 60] are some examples of such studies. We test this assumption below. First, we illustrate some concepts by showing in Fig. 5 a few important quantities and definitions. The total potential energy at a specific shape E_{pot} is the liquid-drop-model energy at this specific shape plus, for the same shape, the shell-plus-pairing correction $E_{\mathrm{s+p}}$ (which is negative

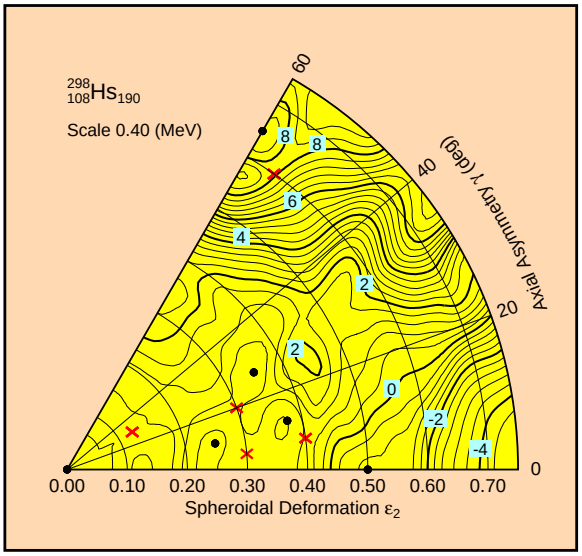

FIG. 8. (Color online) Calculated potential-energy surface for $^{298}_{108}\mathrm{Hs}_{190}$. Local minima are shown by black dots, while saddle points are shown by magenta-colored crosses. The ground state is located at $\gamma = 60$ and $\epsilon_2 = 0.65$, because this is the minimum with the highest barrier with respect to fission, see text for further discussion. But with such a low barrier this isotope would not be observable.

at the ground state in the case here). To obtain manageable numbers we give all energies relative to the spherical liquid-drop energy, including the liquid-drop energy itself. Therefore at a specific deformation β (which is a shorthand for any number of deformation parameters, by definition zero for a sphere)

$$E_{\mathrm{pot}}(\beta) = E_{\mathrm{ld}}(\beta) + E_{\mathrm{s+p}}(\beta) - E_{\mathrm{ld}}(\beta = 0) \qquad (5)$$

The nuclear mass at the ground state is, in our treatment, the sum of E_{pot} at the ground-state minimum and a zero-point energy [33]. Again, this is relative to the spherical liquid-drop mass (or energy) and is often designated "microscopic correction" E_{mic}. The "unnormalized" nuclear mass is therefore the spherical liquid-drop mass plus the microscopic correction. It is thus relative to the potential-energy at the ground state **plus** the zero-point energy that we define the barrier height. By accident the macroscopic barrier B_{ld} is, in this example, almost the same as B_{f}, but generally this is not the case. For ^{208}Pb the difference would be more than 10 MeV due to the large, negative $E_{\mathrm{s+p}}$ at the spherical ground-state shape.

We show in Fig. 6 the differences between our saddle-point energies in the macroscopic-microscopic FRLDM model and the saddle-point energies from our macroscopic FRLDM model, both determined in the same five-dimensional space; of course, the shapes of the saddle points in the two models are different. The difference is, as postulated, fairly small across large regions of the plot. The rms deviation is 2.25 MeV and the mean deviation

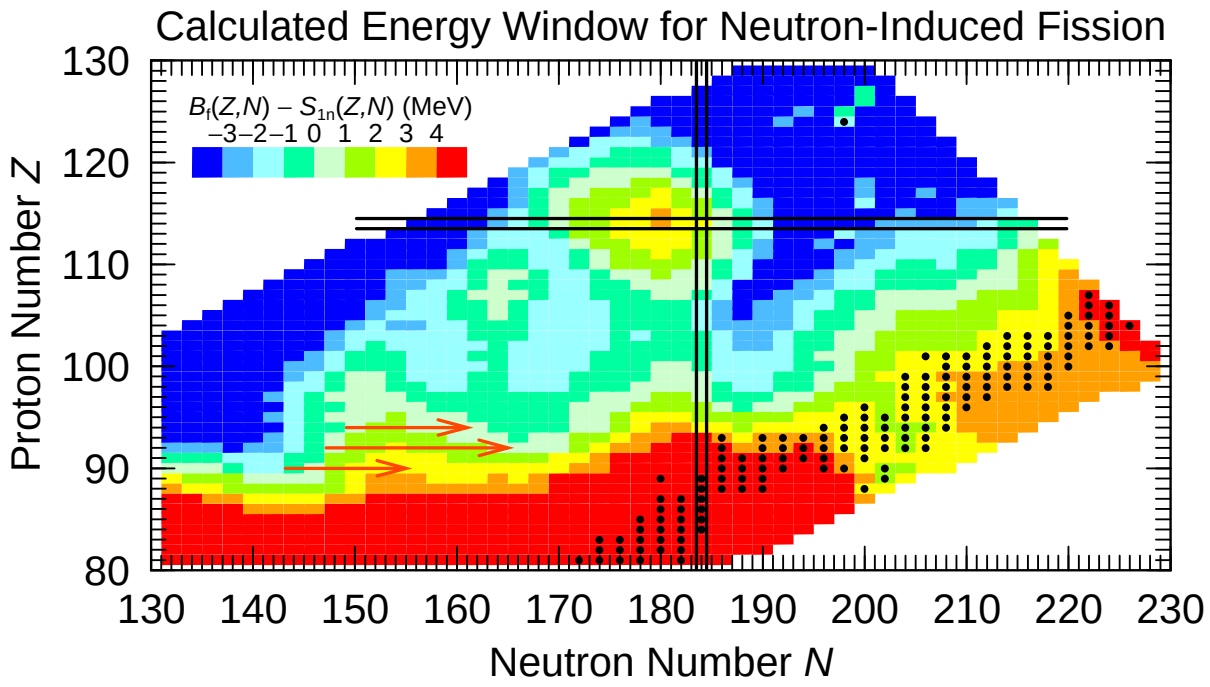

FIG. 9. (Color online) Energy window [7] for neutron-induced fission. The black dots indicate even-N nuclei for which 1.0 MeV $< S_{1n} <$ 2.0 MeV, the so-called r-process boulevard, the region of the chart where the r-process proceeds. If the plotted quantity is negative, the system is unstable with respect to thermal neutron-induced fission. The magenta arrows indicate prompt neutron-capture chains in nuclear weapons tests, see text for further discussion of this and the single outlying dot at $Z = 124$.

(with sign) is −0.78 MeV. In the region of large negative deviations, we find the maximum deviation of −8.45 MeV for $^{171}_{60}$Nd$_{111}$. Why does this large deviation occur here? We calculate the shell-plus-pairing corrections at the saddle-point shape and find it is −8.94 MeV. This saddle-point shape is shown in Fig. 7. It is symmetric and the nascent fragments are spherical. The fragments are near doubly-magic $^{78}_{28}$Ni$_{50}$, which in its ground-state has a shell+pairing correction of −5.89 MeV. (As shown in Fig. 5, the *microscopic correction* tabulated in Ref. [7] is different from this number.) Twice this number makes −11.78 MeV. The shell-plus-pairing correction we obtain at the saddle point is close, but slightly smaller for a number of reasons, mainly the shape is not two well-separated Ni nuclei, and the matter in the nascent fragments corresponds to $Z = 26$ and $N = 48$, if the partial spheres are completed to full spheres; the rest of the matter is outside these completed spheres in the neck region. So we now understand why the macroscopic approximation to the saddle energy is of poor accuracy in this particular region. The fragment shell effects dig a deep valley into the potential energy of the compound system in the neighborhood of the saddle point and lower the potential energy by a substantial amount. One may then ask why this does not happen in the actinide region; why does not the shell effect in the doubly-magic $^{132}_{50}$Sn$_{82}$ (which is −12.82 MeV) affect the saddle-point energy in a similar fashion for actinides? The answer is that the saddle shape of $^{171}_{60}$Nd$_{111}$ is much more elongated; $\beta_2 = 2.40$ for this nuclide whereas for $^{232}_{92}$U$_{140}$ and $^{238}_{92}$U$_{146}$ we find that $\beta_2 = 1.06$ and $\beta_2 = 0.86$, respectively. For $^{171}_{60}$Nd$_{111}$ the saddle shape is very close to the configuration of separated fragments so the fragment shell effects are almost fully present at the saddle point, while for actinides, while these effects may be present, they are not able to be as fully manifested. Also, when the saddle shape is asymmetric, the macroscopic energy is considerably higher than at the macroscopic, mass-symmetric saddle shape, so this increase in the macroscopic energy cancels a considerable fraction of the "fragment" shell effect. When the saddle shape is symmetric, as is the case for $^{171}_{60}$Nd$_{111}$ this does not occur so the fragment shell effects are more visible at a symmetric saddle than at asymmetric saddle shapes.

When the barrier is very low seemingly "pathological" results can be obtained. For example we find for $^{298}_{108}$Hs$_{190}$ that the plotted difference is 7.90 MeV, a very local, surprising, and large deviation. The macroscopic saddle energy is 0.32 MeV and the saddle energy obtained from the macroscopic-microscopic model is 8.22 MeV. To understand these seemingly incompatible results we show in Fig. 8 the calculated potential-energy surface for $^{298}_{108}$Hs$_{190}$, as a function of elongation ϵ_2 and axial asymmetry γ. The details of the calculation and the

coordinates are discussed in Ref. [1]. We showed there that for heavy elements one cannot routinely choose as the ground state the lowest minimum in the potential-energy surface because such a minimum may have a very low barrier with respect to fission. Instead one should choose as the ground state the minimum with the highest barrier with respect to fission, which should have the longest half-life. In this case we identify the minimum at $\epsilon_2 = 0.65$ and $\gamma = 60$ with the ground state and the nearby saddle point indicated by crossed lines, with an energy near 8.2 MeV as the "macroscopic-microscopic" saddle point. Thus we seem to get a very large failure of the method to use the macroscopic saddle-point energy instead of the "exact" saddle-point energy. However, a very small perturbation of the calculated energies could result in, say the minimum at $\epsilon_2 = 0.375$ and $\gamma = 15$ to be identified as the most stable minimum, and the nearby saddle at about 0.8 MeV energy to be the macroscopic-microscopic saddle-point energy, now in good agreement with the macroscopic saddle energy. We can summarize these studies as follows

1. When discussing the macroscopic approximation to the saddle energy, it is not meaningful to consider nuclei with fission barriers that are so low they would be too unstable to exist. Fig. 1 shows that most nuclei slightly above $N = 184$ fall in this category, with some interesting exceptions for low Z and large N.

2. Above $Z = 80$ and $N \leq 184$ the rms deviation between the exact and macroscopic model is 1.12 MeV for the 2433 nuclei in this restricted region. The mean deviation is +0.19 MeV. If all nuclei are included the rms deviation is 2.25 MeV and the mean deviation −0.78 MeV, mainly due to the very large negative deviations near $^{171}_{60}\mathrm{Nd}_{111}$.

3. For systems with $Z < 80$ the macroscopic approximation to the saddle potential energy becomes increasingly inaccurate as Z becomes lower.

4. Although the macroscopic saddle energy in some regions is a good approximation to the saddle energy obtained in the macroscopic-microscopic model, the shapes associated with the saddle points are very poor approximations to shapes obtained in realistic models. To model fission properties such as low-energy fission-fragment mass distributions, potential-energy surfaces of at least five dimensions calculated either in a macroscopic-microscopic model or some other model with realistic microscopic shell structure are necessary [37–39].

We desire to investigate the accuracy of the calculated barrier heights for neutron-rich nuclei with the aim of understanding their suitability for use in studies such as fission at the end of the r-process. Unfortunately, there are no large-scale systematic experimental studies of fission properties for large regions of nuclei on the neutron-rich side of β stability. However, some indirect results are available. The r-process can be approximately simulated in certain nuclear explosions through a process called "prompt neutron capture". It is called prompt because the timescale of the neutron fluence is nanoseconds rather than the seconds time scale of the r-process, so the processes are not fully equivalent; no β-decay can occur during the prompt capture due to its short timescale. For a comprehensive discussion of these experiments see Ref. [61]. Because no β-decay takes place during neutron capture the process, with some qualifications [61], proceeds along an isotope chain, successively producing increasingly neutron-rich isotopes of a specific element. One necessary condition for the capture sequence to proceed is that the fission barrier be higher than the neutron-separation energy in the compound system following neutron capture. We investigate if our calculations are consistent with experimental observations as regards this necessary condition. In Fig. 9 we show the difference between calculated barrier heights and calculated neutron-separation energies for even systems. Odd compound systems have a (slightly) higher fission barrier and lower neutron-separation energies so they are irrelevant for locating the termination of the capture sequence. Also shown, with magenta arrows, are the "observed" range of neutron-capture chains on the targets $^{232}_{90}\mathrm{Th}_{142}$, $^{238}_{92}\mathrm{U}_{146}$, and $^{242}_{94}\mathrm{Pu}_{148}$. In the uranium chain $^{257}_{92}\mathrm{U}_{165}$ is reached. This conclusion is not reached by recovering $^{257}_{92}\mathrm{U}_{165}$ in the debris from the explosion, as it has a calculated β-decay half-life of about 0.5 s [62], too short to allow recovery. Rather, one observes higher-Z, less neutron-rich elements at the endpoint of β-decay chains from the original isotopes in the capture chain. The termination point of the neutron-capture chain is deduced from the highest A-value observed in these groups of nuclei.

From Fig. 9 we see that the observed capture chains for the $^{238}_{92}\mathrm{U}_{146}$ and $^{242}_{94}\mathrm{Pu}_{148}$ targets terminate exactly where the plotted function goes below zero, that is, where the fission-barrier height becomes lower than the neutron separation energy, which would result in termination of the capture sequence by fission. Therefore, the calculated results are consistent with these observations. The capture chain on the $^{232}_{90}\mathrm{Th}_{142}$ target terminates before zero is reached, but it is argued [61] that this is because the capture cross sections in this chain are very low. So both our calculated barrier heights and neutron separation energies are consistent with this set of experimental data.

There also could be other mechanisms that cause no nuclei heavier than $A = 257$ to be observed. Nuclei near proton number $Z = 100$ and neutron number $N = 164$ have unusually short half-lives, see [63, 64] for a review and references to original work. The proposed mechanisms for these short half-lives are two-fold: 1) a very thin barrier due to "erosion" of the outer barrier due to

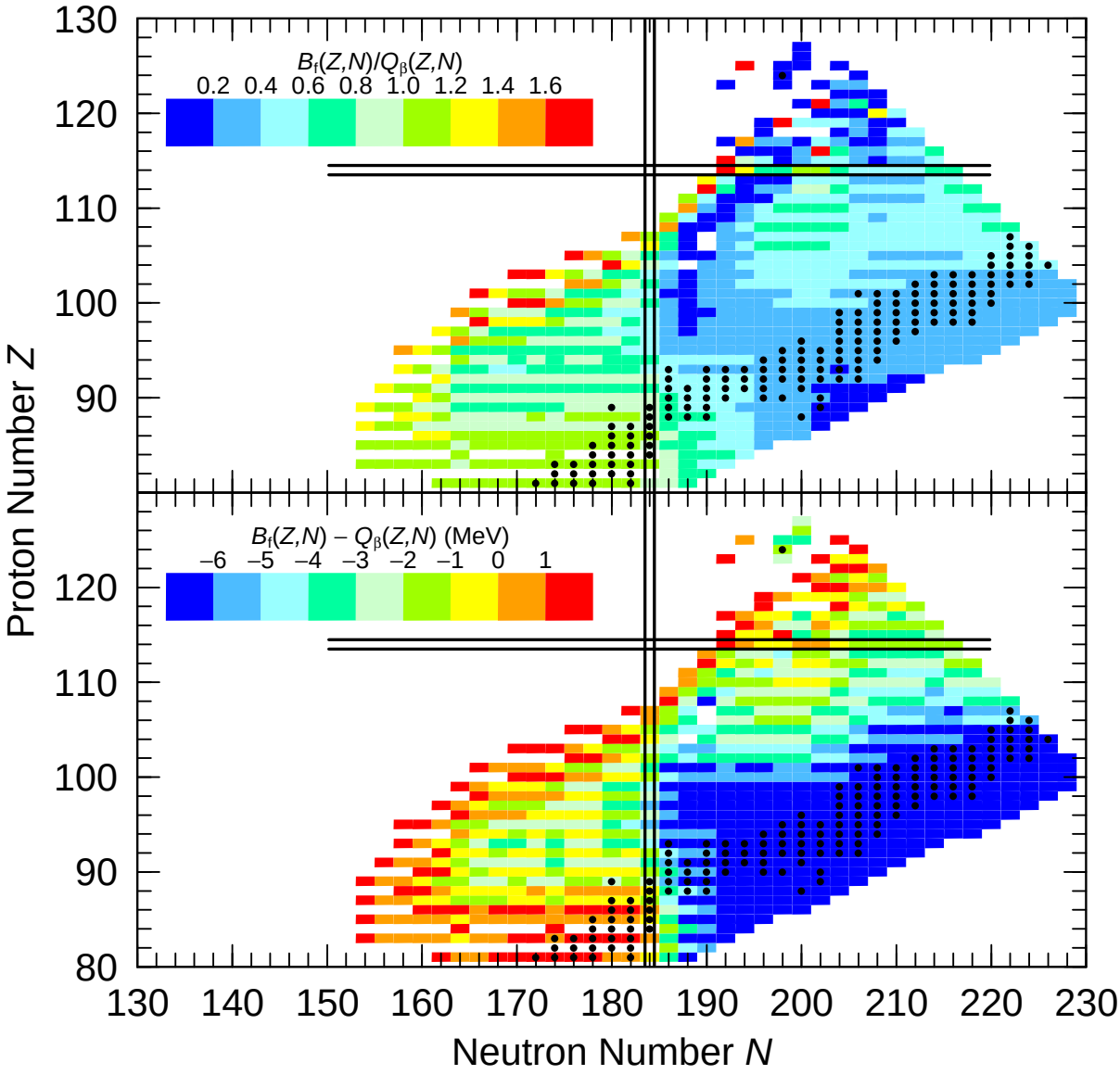

FIG. 10. (Color online) Illustration of quantities affecting β-delayed fission, namely the ratio B_f/Q_β (upper panel) and $B_f - Q_\beta$ (lower panel). Only nuclides for which $B_f - Q_\beta < 2$ MeV are shown. The solid black dots are the same as in Fig. 9, illustrating the "r-process boulevard."

the large shell effects associated with two near-doubly-magic fragments in the vicinity of $^{132}_{50}Sn_{82}$ and 2) effects from the large shell gaps on the mass parameter associated with fission. Both these principles were discussed very early in Ref. [65] and later somewhat more quantitatively in Refs. [6, 28, 66]. Not much data is available for nuclei in this region but we know for Fm there is a sudden drop in half-life 6 nucleons (in this case only neutrons) away from $^{264}_{100}Fm_{164}$ when we approach this nucleus which corresponds to doubly-magic configurations in both daughter fission fragments in symmetric fission. Since fragment ground-state microscopic corrections near $^{132}_{50}Sn_{82}$ decrease in a similar fashion with proton and neutron number variation we may as a rule of thumb anticipate that very short fission half-lives occur at

$$|100 - Z| + |164 - N| \leq 6. \quad (6)$$

Thus even if the actual barriers are higher than the values obtained in our calculations and the capture chain proceeds all the way to $A = 270$ there would be no β-stable products following decay towards stability because the β-decay chains would terminate in fission before relatively stable elements are reached. For instance, suppose $^{260}_{92}U_{168}$ is reached. When it decays back, according to the above condition $^{260}_{95}Am_{165}$ would terminate the decay chain by fission. The precursor

$^{260}_{94}Pu_{166}$ has a calculated β-decay half-life of 0.8 s [62], too short to recover this hypothetical isotope.

In Fig. 9 we have marked even-N nuclides with 1 MeV $< S_{1n} <$ 2 MeV with black dots, defining what is referred to as the r-process boulevard. Along the boulevard the neutron-separation energy is lower than the barrier (although *closer* to stability this is not the case), so according to the results here the r-process can proceed to the heaviest region along this boulevard. However during β-decay back to stability the decay paths will enter regions with very low barriers so some of the nuclides here will have spontaneous fission half-lives in the microsecond range or lower.

We note that the isolated black dot, indicating that the nuclide at $Z = 124$ and $N = 198$ satisfies the condition which defines the "r-process boulevard," is caused by the phenomenon of highly varying deformations of the ground states in neighboring highly unstable isotopes, due to effects similar to those discussed in reference to Fig. 8.

When the β-decay Q_β value is higher than the fission barrier in the daughter, which is the case across a large region of neutron-rich heavy nuclei, β-delayed fission can occur, sometimes with a high probability. This is illustrated in Fig. 10. The ratio between the barrier height and Q_β is shown in the top panel. Only nuclides for which $B_f - Q_\beta < 2$ MeV are shown, because for decays to energies more than 2 MeV below the barrier peak the delayed fission branch is negligible. Spontaneous fission from the ground state may still occur with a high probability. Smaller ratios correspond to higher probability of delayed fission. As a complementary view we present in the lower panel the magnitude of the energy window for β-delayed fission. However the branching ratio for β-delayed fission is not directly related to the magnitude of this window. For example in a decay with a barrier height of, say, $B_f = 2$ MeV and $Q_\beta = 6$ MeV the branching ration for delayed fission would normally be much larger than if $B_f = 6$ MeV and $Q_\beta = 10$ MeV although the energy window for delayed fission is 4 MeV in both of these situations.

In summary, we have benchmarked, both previously and in this work, our potential-energy-surface calculations and associated predicted nuclear properties with respect to

- barrier heights from $^{70}_{34}Se_{36}$ to $^{252}_{98}Cf_{154}$ [2],
- nuclear ground-state masses [2],
- actinide "double-humped" fission-barrier parameters [1],
- EC-delayed fission data [1, 45, 46],
- spontaneous-fission properties in the heavy-element region,
- fission-fragment charge-yield data for 70 nuclides [39],
- some prompt neutron-capture data obtained in weapons tests.

These studies have been consistently encouraging and represent quite diverse tests, which show that the calculated potential-energy surfaces give a realistic description of available experimental data, including in regions of the nuclear chart far removed from regions considered in determining the parameters of the model. It therefore seems to be very timely to incorporate this calculated fission-barrier-height data base in studies of fission in the r-process. Such studies would require a sophisticated network that should include pathways and branching ratios for neutron capture, neutron-induced fission, β-decay, β-delayed fission, and spontaneous fission. In the fission branches, ideally the fission-fragment yields should also be included.

This work was supported by travel grants for P.M. to JUSTIPEN (Japan-U.S. Theory Institute for Physics with Exotic Nuclei) under grant number DE-FG02-06ER41407 (U. Tennessee). This work was carried out under the auspices of the National Nuclear Security Administration of the U.S. Department of Energy at Los Alamos National Laboratory under Contract No. DE-AC52-06NA25396. TI was supported in part by MEXT SPIRE and JICFuS and JSPS KAKENHI Grant no. 25287065. MM was supported by the Notre Dame Joint Institute for Nuclear Astrophysics, NSF grant no. PHY0822648.

[1] P. Möller, A. J. Sierk, T. Ichikawa, A. Iwamoto, R. Bengtsson, H. Uhrenholt, and S. Åberg, Phys. Rev. C **79**, 064304 (2009).
[2] P. Möller, A. J. Sierk, and A. Iwamoto, Phys. Rev. Lett. **92**, 072501 (2004).
[3] P. Möller and A. Iwamoto, Proc. Conf. on Nuclear Shapes and Motions. Symposium in Honor of Ray Nix, 25–27 Oct. 1998, Sante Fe, NM, USA Acta Physica Hungarica, New Series, **10**, 241 (1999).
[4] P. Möller and A. Iwamoto, Phys. Rev. C **61**, 047602 (2000).
[5] P. Möller, D. G. Madland, A. J. Sierk, and A. Iwamoto, Tours 2000, Tours Symposium on Nuclear Physics IV, Tours, France September 4–7, 2000, and AIP Conference Proceedings **561**, p. 455 (2001).
[6] P. Möller, D. G. Madland, A. J. Sierk, and A. Iwamoto, Nature **409**, 785 (2001).
[7] P. Möller, J. R. Nix, W. D. Myers, and W. J. Swiatecki, Atomic Data Nucl. Data Tables **59**, 185 (1995).
[8] S. Ćwiok, W Nazarewicz, J. X. Saladin, W. Plociennik, A. Johnson, Phys. Lett. **B322**, 304 (1994).
[9] G. M. Ter-Akopian, J. H. Hamilton, Y. T. Oganessian, A. V. Daniel, J. Kormicki, A. V.Ramayya, G. S. Popeko, B. R. S. Babu, Q. H. Lu, K. Butlermoore, W. C. Ma, S. Ćwiok, W. Nazarewicz, J. K. Deng, D.. Shi, J. Kliman, M. Morhac, J. D. Cole, R. Aryaeinejad, N. R. Johnson, I. Y. Lee, F. K. McGowan, J. X. Saladin, Phys. Rev. Lett. **77**, 32 (1996).
[10] A. Sobiczewski, P. Jachimowicz, and M. Kowal, Int. J. Mod. Phys. E-Nucl. Phys. **19**, 493 (2010).
[11] P. Jachimowicz, M. Kowal, and J. Skalski, Phys. Rev. C **85**, 034305 (2012).
[12] H, Flocard, P. Quentin, A. K. Kerman, D, Vautherin,. Nucl. Phys. **A203**, 433 (1973).
[13] B. Hayes, Am. Sci. **88**, 481 (2000).
[14] N. Dubray, D. Regnier, Comp. Phys. Comm. **183**, 2035 (2012).
[15] S. G. Nilsson, Kgl. Danske Videnskab. Selskab. Mat.-Fys. Medd. **29**:No. 16 (1955).
[16] S. G. Nilsson, C. F. Tsang, A. Sobiczewski, Z. Szymański, S. Wycech, C. Gustafson, I.-L. Lamm, P. Möller, and B. Nilsson, Nucl. Phys. **A131** (1969) 1.
[17] S. Ćwiok, J. Dudek, W Nazarewicz, J. Skalski, and T. Werner, Comput. Phys. Commun. **46** 379 (1987).
[18] M. Bolsterli, E. O. Fiset, J. R. Nix, and J. L. Norton, Phys. Rev. C **5** (1972) 1050.
[19] H. J. Krappe, J. R. Nix, and A. J. Sierk, Phys. Rev. C **20** (1979) 992.
[20] W. D. Myers and W. J. Swiatecki, Nucl. Phys. **81** (1966) 1.
[21] W. D. Myers and W. J. Swiatecki, Ark. Fys. **36** (1967) 343.
[22] K. T. R. Davies, A. J. Sierk, and J. R. Nix, Phys. Rev. C **13** (1976) 2385.
[23] N. Bohr and J. A. Wheeler, Phys. Rev. **56** (1939) 426.
[24] O. Hahn and F. Strassmann, Naturwiss. **27** (1939) 11.
[25] L. Meitner and O. R. Frisch, Nature **143** (1939) 239.
[26] O. R. Frisch, Nature **143** (1939) 276.
[27] H. A. Bethe and R. F. Bacher, Rev. Mod. Phys. **8** 82 (1936).
[28] P. Möller, J. R. Nix, and W. J. Swiatecki, Nucl. Phys. **A492**, 349 (1989).
[29] W. D. Myers and W. J. Swiatecki, Ann. Phys. (N. Y.) **55** (1969) 395.
[30] P. Möller and J. R. Nix, Proc. Third IAEA Symp. on the physics and chemistry of fission, Rochester, 1973, vol. I (IAEA, Vienna, 1974) p. 103.
[31] P. Möller and J. R. Nix, Nucl. Phys. **A229** (1974) 269.
[32] P. Möller, S. G. Nilsson, and J. R. Nix, Nucl. Phys. **A229** (1974) 292.
[33] P. Möller and J. R. Nix, Nucl. Phys. **A361**, 117 (1981).
[34] P. Möller and J. R. Nix, Nucl. Phys. **A536** (1992) 20.
[35] P. Möller and S. G. Nilsson, Phys. Lett. **31B** (1970) 283.
[36] L. Wilets, Theories of nuclear fission (Clarendon Press, Oxford, 1964).
[37] J. Randrup and P. Möller, Phys. Rev. Lett. **106**, 132503 (2011).
[38] J. Randrup, P. Möller, and A. J. Sierk, Phys. Rev. C **84**, 034613 (2011).
[39] J. Randrup and P. Möller, Phys. Rev. C **88**, 064606 (2013).
[40] J. Blons, R Fabbro, C. Mazur, D. Paya, M. Ribrag, Y. Patin, Nucl. Phys. **A477**, 231 (1988).
[41] T. Ichikawa, P. Möller, and A. J. Sierk, Phys. Rev. C **87**, 054326 (2013).
[42] L. Csige, M. Csatlós, T. Faestermann, Z. Gácsi, J. Gulyás, D. Habs, R. Hertenberger, A. Krasznahorkay, R. Lutter, H. J. Maier. P. G. Thirolf, H.-F. Wirth, Phys. Rev. C **80**, 054306 (2009).
[43] L. Csige, M. Csatlós, T. Faestermann, J. Gulyás, D. Habs, R. Hertenberger, M. Hunyadi, A. Krasznahorkay, H. J. Maier, P. G. Thirolf, H.-F. -Wirth, Phys. Rev. C **85**, 054306 (2012).
[44] L. Csige, D. M. Filipescu, T. Glodariu, J. Gulyás, M. M. Günther, D. Habs, H. J. Karwowski, A. Krasznahorkay, G. C Rich, M. Sin, L. Stroe, O.Tesileunu, and P. G. Thirolf, Phys. Rev. C **87**, 044321 (2013).
[45] A. N. Andreyev M. Huyse, and P. Van Duppen, Rev. Mod. Phys. **85**, 1541 (2013).
[46] M. Veselský, A. N. Andreyev, S.Antalic, M. Huyse, P. Möller, K. Nishio, A. J. Sierk, P. Van Duppen, and M. Venhart, Phys. Rev. C **86**, 024308 (2012).
[47] W. J. Swiatecki, Phys. Rev. **100**, 937 (1955).
[48] Z. Patyk, A. Sobiczewski, P. Armbruster and K.-H. Schmidt, Nucl. Phys. **A491**, 267 (1989).
[49] J. Randrup, C. F. Tsang, P. Möller, S. G. Nilsson, and S. E. Larsson, Nucl. Phys. **A217**, 221 (1973).
[50] J. Randrup, S. E. Larsson, P. Möller, S. G. Nilsson, K. Pomorski, and A. Sobiczewski, Phys. Rev. C **13**, 229 (1976).
[51] A. Baran, K. Pomorski, A. Łukasiak, and A. Sobiczewski, Nucl. Phys. **A361**, 83 (1981).
[52] A. Staszczak, A. Baran, J. Dobaczewski, and W. Nazarewicz, Phys. Rev. C **80**, 014309 (2009).
[53] A. Baran, A. Staszczak, and W. Nazarewicz, Int. J. Mod. Phys. E **20**, 557 (2011).
[54] B. B. Back, O. Hansen, H. C. Britt, and J. D. Garrett, Phys. Rev. C **9** (1974) 1924.
[55] B. B. Back, H. C. Britt, O. Hansen, B. Leroux, and J. D. Garrett, Phys. Rev. C **10** (1974) 1948.
[56] H. C. Britt, Proc. 4th IAEA Symp. on physics and chemistry of fission, Jülich, 1979, vol. I (IAEA, Vienna, 1980)

p. 3.
[57] S. Bjørnholm and J. E. Lynn, Rev. Mod. Phys. **52** (1980) 725.
[58] G. Henning1, A. Lopez-Martens , T.L. Khoo, D. Seweryniak, M. Alcorta, M. Asai, B. B. Back, P. Bertone, D. Boilley, M. P. Carpenter, C. J. Chiara, P. Chowdhury, B. Gall, P. T. Greenlees, G. Gurdal, K. Hauschild, A. Heinz, C. R. Hoffman, R. V. F. Janssens, A. V. Karpov, B. P. Kay, F. G. Kondev, S. Lakshmi, T. Lauristen, C. J. Lister, E. A. McCutchan, C. Nair, J. Piot, D. Potterveld, P. Reiter1, N. Rowley, A. M. Rogers, and S. Zhu, EPJ Web of Conferences **66** 02046 (2014).
[59] S. Hofmann, Superheavy Nuclei, in Encyclopedia of Nuclear Physics and its Application, Edited by Reinhard Stock, Wiley-VCH Verlag GmbH & Co., Weinheim, Germany, 2013, pp. 213–246.
[60] W. D. Myers and W. J. Swiatecki, Nucl. Phys. **A612**, 249 (1997).
[61] S. A. Becker, Carnegie Observatories Astrophysics Series, Vol 4, Origin and Evolution of the Elements, 2003, ed. A. McWilliam and M. Rauch (Pasadena: Carnegie Observatories, URL:
symposia.obs.carnegiescience.edu/series/symposium4
/ms/becker.ps.gz.
[62] P. Möller, J. R. Nix, and K.-L. Kratz, Atomic Data Nucl. Data Tables **66**, 131 (1997).
[63] N. E. Holden and D. C. Hoffman, Pure and Appl. Chem. **72**, 1525 (2000).
[64] N. E. Holden and D. C. Hoffman, Pure and Appl. Chem. **73**, 1225 (2001).
[65] U. Mosel and H. W. Schmitt, Phys. Rev. C **4**, 2185 (1971).
[66] P. Möller, J. R. Nix, and W. J. Swiatecki, Nucl. Phys. **A469**, 1 (1987).

TABLE I. Calculated Fission-Barrier Heights

N	A	$B_{\rm f}$ (MeV)	N	A	$B_{\rm f}$ (MeV)	N	A	$B_{\rm f}$ (MeV)	N	A	$B_{\rm f}$ (MeV)	N	A	$B_{\rm f}$ (MeV)	N	A	$B_{\rm f}$ (MeV)
$Z = 51$ (Sb)			**$Z = 55$ (Cs)**			**$Z = 57$ (La)**			**$Z = 59$ (Pr)**			**$Z = 60$ (Nd)**			**$Z = 62$ (Sm)**		
120	171	42.48	127	182	43.33	133	190	36.61	126	185	41.88	140	200	30.76	114	176	32.07
121	172	43.34	128	183	42.12	134	191	35.39	127	186	40.92	141	201	30.58	115	177	32.50
$Z = 52$ (Te)			129	184	40.77	135	192	34.28	128	187	39.73	**$Z = 61$ (Pm)**			116	178	32.59
119	171	41.24	130	185	39.26	**$Z = 58$ (Ce)**			129	188	38.62	110	171	32.33	117	179	33.13
120	172	41.73	**$Z = 56$ (Ba)**			113	171	34.22	130	189	37.41	111	172	32.25	118	180	33.70
121	173	42.63	115	171	36.71	114	172	34.49	131	190	36.98	112	173	32.25	119	181	34.11
122	174	43.12	116	172	37.22	115	173	35.20	132	191	36.05	113	174	32.54	120	182	34.47
123	175	43.87	117	173	37.85	116	174	35.47	133	192	35.47	114	175	32.62	121	183	35.41
124	176	44.38	118	174	38.29	117	175	36.41	134	193	34.50	115	176	32.91	122	184	35.94
$Z = 53$ (I)			119	175	39.14	118	176	36.76	135	194	34.11	116	177	33.10	123	185	36.97
118	171	40.35	120	176	39.32	119	177	37.42	136	195	33.15	117	178	33.84	124	186	37.62
119	172	41.42	121	177	40.20	120	178	37.81	137	196	32.54	118	179	34.27	125	187	38.94
120	173	41.76	122	178	40.39	121	179	38.62	138	197	31.96	119	180	35.04	126	188	39.36
121	174	42.43	123	179	41.29	122	180	39.05	139	198	31.33	120	181	35.28	127	189	38.37
122	175	42.68	124	180	41.75	123	181	39.94	**$Z = 60$ (Nd)**			121	182	36.40	128	190	37.42
123	176	43.56	125	181	43.23	124	182	40.59	111	171	32.65	122	183	36.83	129	191	36.23
124	177	43.98	126	182	43.36	125	183	41.89	112	172	32.73	123	184	37.96	130	192	35.28
125	178	45.53	127	183	42.27	126	184	42.24	113	173	32.98	124	185	38.61	131	193	34.85
126	179	45.87	128	184	41.25	127	185	41.23	114	174	33.24	125	186	40.01	132	194	33.81
$Z = 54$ (Xe)			129	185	39.85	128	186	40.17	115	175	33.50	126	187	40.36	133	195	33.16
117	171	38.87	130	186	38.40	129	187	38.83	116	176	33.73	127	188	39.42	134	196	32.07
118	172	39.50	131	187	37.68	130	188	37.53	117	177	34.54	128	189	38.44	135	197	31.44
119	173	40.40	132	188	36.74	131	189	36.93	118	178	35.10	129	190	37.31	136	198	31.00
120	174	40.77	133	189	36.60	132	190	36.19	119	179	35.83	130	191	36.28	137	199	30.93
121	175	41.43	**$Z = 57$ (La)**			133	191	35.72	120	180	36.02	131	192	35.87	138	200	30.66
122	176	41.72	114	171	35.64	134	192	35.01	121	181	36.89	132	193	34.87	139	201	30.52
123	177	42.51	115	172	36.24	135	193	34.02	122	182	37.44	133	194	34.23	140	202	30.26
124	178	42.94	116	173	36.81	136	194	33.09	123	183	38.51	134	195	33.15	141	203	30.29
125	179	44.48	117	174	37.36	137	195	32.25	124	184	39.11	135	196	32.48	142	204	30.33
126	180	44.73	118	175	37.79	**$Z = 59$ (Pr)**			125	185	40.47	136	197	31.89	143	205	30.33
127	181	43.46	119	176	38.61	112	171	33.38	126	186	40.86	137	198	31.82	144	206	30.23
128	182	42.04	120	177	39.04	113	172	33.74	127	187	39.83	138	199	31.43	145	207	29.96
$Z = 55$ (Cs)			121	178	39.79	114	173	33.91	128	188	38.86	139	200	31.15	146	208	29.63
116	171	38.23	122	179	40.18	115	174	34.32	129	189	37.60	140	201	30.91	**$Z = 63$ (Eu)**		
117	172	38.95	123	180	41.01	116	175	34.61	130	190	36.51	141	202	30.78	108	171	32.51
118	173	39.34	124	181	41.50	117	176	35.62	131	191	35.97	142	203	30.74	109	172	32.61
119	174	40.13	125	182	42.90	118	177	36.09	132	192	35.02	143	204	30.85	110	173	31.96
120	175	40.44	126	183	43.20	119	178	36.76	133	193	34.46	144	205	30.55	111	174	31.87
121	176	41.34	127	184	42.20	120	179	37.19	134	194	33.43	**$Z = 62$ (Sm)**			112	175	31.62
122	177	41.47	128	185	40.94	121	180	38.03	135	195	32.65	109	171	32.27	113	176	31.80
123	178	42.31	129	186	39.77	122	181	38.50	136	196	31.85	110	172	32.19	114	177	31.67
124	179	42.71	130	187	38.41	123	182	39.57	137	197	32.09	111	173	31.96	115	178	31.98
125	180	44.24	131	188	37.79	124	183	40.13	138	198	31.61	112	174	32.04	116	179	32.15
126	181	44.51	132	189	36.97	125	184	41.47	139	199	30.94	113	175	32.15	117	180	32.66

TABLE I. (*Continued*)

N	A	$B_{\rm f}$ (MeV)	N	A	$B_{\rm f}$ (MeV)	N	A	$B_{\rm f}$ (MeV)	N	A	$B_{\rm f}$ (MeV)	N	A	$B_{\rm f}$ (MeV)	N	A	$B_{\rm f}$ (MeV)
$Z = 63$ (Eu)			**$Z = 64$ (Gd)**			**$Z = 65$ (Tb)**			**$Z = 66$ (Dy)**			**$Z = 66$ (Dy)**			**$Z = 67$ (Ho)**		
118	181	33.01	119	183	33.06	117	182	31.92	111	177	31.19	155	221	26.53	146	213	28.43
119	182	33.62	120	184	33.53	118	183	32.08	112	178	30.85	**$Z = 67$ (Ho)**			147	214	28.19
120	183	34.06	121	185	34.13	119	184	32.51	113	179	30.65	104	171	31.25	148	215	28.10
121	184	34.93	122	186	34.52	120	185	32.94	114	180	30.60	105	172	31.49	149	216	28.10
122	185	35.36	123	187	35.37	121	186	33.67	115	181	31.05	106	173	31.15	150	217	28.04
123	186	36.33	124	188	35.91	122	187	33.93	116	182	31.01	107	174	31.57	151	218	27.99
124	187	36.90	125	189	37.25	123	188	34.78	117	183	31.43	108	175	31.40	152	219	27.53
125	188	38.37	126	190	37.70	124	189	35.25	118	184	31.58	109	176	31.71	153	220	27.26
126	189	38.73	127	191	36.64	125	190	36.39	119	185	31.99	110	177	31.30	154	221	26.79
127	190	37.75	128	192	35.74	126	191	36.97	120	186	32.39	111	178	30.91	155	222	26.52
128	191	36.78	129	193	34.77	127	192	35.86	121	187	32.99	112	179	30.42	156	223	26.09
129	192	35.84	130	194	33.84	128	193	34.90	122	188	33.15	113	180	30.36	157	224	25.73
130	193	34.82	131	195	33.45	129	194	34.12	123	189	33.86	114	181	30.28	**$Z = 68$ (Er)**		
131	194	34.65	132	196	32.43	130	195	32.99	124	190	34.37	115	182	30.61	103	171	32.34
132	195	33.47	133	197	31.80	131	196	32.72	125	191	35.51	116	183	30.55	104	172	31.21
133	196	32.85	134	198	30.83	132	197	31.76	126	192	36.05	117	184	31.09	105	173	31.27
134	197	31.75	135	199	30.35	133	198	31.19	127	193	34.88	118	185	31.04	106	174	31.02
135	198	31.29	136	200	30.00	134	199	30.32	128	194	34.06	119	186	31.43	107	175	30.51
136	199	30.83	137	201	29.98	135	200	29.99	129	195	33.15	120	187	31.81	108	176	30.37
137	200	30.83	138	202	29.82	136	201	29.63	130	196	32.08	121	188	32.43	109	177	30.27
138	201	30.55	139	203	29.61	137	202	29.83	131	197	31.55	122	189	32.56	110	178	30.10
139	202	30.50	140	204	29.60	138	203	29.60	132	198	30.57	123	190	33.44	111	179	29.80
140	203	30.25	141	205	29.45	139	204	29.55	133	199	29.99	124	191	33.68	112	180	29.36
141	204	30.34	142	206	29.60	140	205	29.49	134	200	29.22	125	192	34.82	113	181	29.60
142	205	30.37	143	207	29.58	141	206	29.40	135	201	28.88	126	193	35.31	114	182	29.88
143	206	30.39	144	208	29.58	142	207	29.45	136	202	28.60	127	194	34.28	115	183	29.85
144	207	30.24	145	209	29.50	143	208	29.60	137	203	28.79	128	195	33.32	116	184	30.04
145	208	30.04	146	210	29.12	144	209	29.55	138	204	28.64	129	196	32.30	117	185	30.28
146	209	29.70	147	211	29.00	145	210	29.57	139	205	28.55	130	197	31.22	118	186	30.44
147	210	29.56	148	212	28.75	146	211	29.16	140	206	28.46	131	198	30.66	119	187	30.90
148	211	29.37	149	213	28.85	147	212	29.07	141	207	28.43	132	199	29.73	120	188	31.35
$Z = 64$ (Gd)			150	214	28.69	148	213	28.69	142	208	28.47	133	200	29.29	121	189	31.74
107	171	32.85	**$Z = 65$ (Tb)**			149	214	28.98	143	209	28.65	134	201	28.56	122	190	31.80
108	172	32.49	106	171	33.01	150	215	28.72	144	210	28.65	135	202	28.43	123	191	32.55
109	173	32.33	107	172	32.80	151	216	28.62	145	211	28.73	136	203	28.19	124	192	32.98
110	174	31.92	108	173	32.60	152	217	28.31	146	212	28.54	137	204	28.44	125	193	34.15
111	175	31.71	109	174	32.17	153	218	27.84	147	213	28.27	138	205	28.23	126	194	34.51
112	176	31.47	110	175	31.84	**$Z = 66$ (Dy)**			148	214	28.20	139	206	28.58	127	195	33.46
113	177	31.30	111	176	31.41	105	171	32.57	149	215	28.21	140	207	28.41	128	196	32.72
114	178	31.27	112	177	30.95	106	172	31.84	150	216	28.13	141	208	28.26	129	197	31.55
115	179	31.72	113	178	30.99	107	173	32.35	151	217	28.02	142	209	28.25	130	198	30.32
116	180	31.66	114	179	30.91	108	174	32.39	152	218	27.62	143	210	28.47	131	199	29.56
117	181	32.20	115	180	31.31	109	175	31.98	153	219	27.28	144	211	28.47	132	200	28.59
118	182	32.59	116	181	31.43	110	176	31.55	154	220	26.84	145	212	28.56	133	201	28.07

TABLE I. (*Continued*)

N	A	$B_{\rm f}$ (MeV)	N	A	$B_{\rm f}$ (MeV)	N	A	$B_{\rm f}$ (MeV)	N	A	$B_{\rm f}$ (MeV)	N	A	$B_{\rm f}$ (MeV)	N	A	$B_{\rm f}$ (MeV)
$Z = 68$ (Er)			**$Z = 69$ (Tm)**			**$Z = 70$ (Yb)**			**$Z = 70$ (Yb)**			**$Z = 71$ (Lu)**			**$Z = 72$ (Hf)**		
134	202	27.42	119	188	30.00	102	172	29.20	146	216	26.08	124	195	31.26	100	172	24.65
135	203	27.23	120	189	30.75	103	173	29.89	147	217	26.04	125	196	32.25	101	173	25.30
136	204	27.05	121	190	31.09	104	174	29.84	148	218	25.86	126	197	32.57	102	174	25.84
137	205	27.23	122	191	31.18	105	175	30.22	149	219	26.04	127	198	31.67	103	175	26.52
138	206	27.04	123	192	31.93	106	176	30.19	150	220	25.87	128	199	30.75	104	176	27.09
139	207	27.31	124	193	32.45	107	177	30.47	151	221	25.89	129	200	29.36	105	177	27.59
140	208	27.25	125	194	33.61	108	178	30.35	152	222	25.68	130	201	28.10	106	178	28.21
141	209	27.21	126	195	34.02	109	179	30.07	153	223	25.53	131	202	26.98	107	179	28.92
142	210	27.24	127	196	32.84	110	180	29.82	154	224	25.32	132	203	26.05	108	180	28.72
143	211	27.29	128	197	32.02	111	181	29.45	155	225	25.19	133	204	25.53	109	181	28.93
144	212	27.42	129	198	30.82	112	182	28.91	156	226	24.80	134	205	24.99	110	182	28.65
145	213	27.50	130	199	29.50	113	183	28.54	157	227	24.64	135	206	24.73	111	183	28.75
146	214	27.55	131	200	28.76	114	184	28.44	158	228	24.12	136	207	24.36	112	184	28.07
147	215	27.31	132	201	27.86	115	185	28.48	159	229	24.02	137	208	24.53	113	185	27.64
148	216	27.19	133	202	27.41	116	186	28.34	160	230	23.66	138	209	24.35	114	186	27.24
149	217	27.23	134	203	26.74	117	187	28.55	161	231	23.58	139	210	24.62	115	187	26.98
150	218	27.20	135	204	26.59	118	188	28.71	162	232	23.32	140	211	24.58	116	188	26.90
151	219	27.08	136	205	26.35	119	189	29.08	163	233	23.07	141	212	25.11	117	189	27.01
152	220	26.76	137	206	26.57	120	190	29.91	164	234	22.38	142	213	25.05	118	190	27.44
153	221	26.49	138	207	26.47	121	191	30.48	**$Z = 71$ (Lu)**			143	214	25.44	119	191	27.71
154	222	26.14	139	208	26.78	122	192	30.70	100	171	26.54	144	215	25.46	120	192	28.61
155	223	26.00	140	209	26.59	123	193	31.42	101	172	27.28	145	216	25.63	121	193	29.30
156	224	25.64	141	210	27.07	124	194	31.94	102	173	27.65	146	217	25.63	122	194	29.61
157	225	25.34	142	211	26.98	125	195	32.93	103	174	28.42	147	218	25.69	123	195	30.32
158	226	24.80	143	212	27.07	126	196	33.36	104	175	28.92	148	219	25.51	124	196	30.80
159	227	24.50	144	213	27.14	127	197	32.30	105	176	29.42	149	220	25.68	125	197	31.65
$Z = 69$ (Tm)			145	214	27.19	128	198	31.37	106	177	29.54	150	221	25.50	126	198	32.03
102	171	30.81	146	215	27.33	129	199	29.98	107	178	29.86	151	222	25.63	127	199	31.12
103	172	31.28	147	216	27.15	130	200	28.77	108	179	29.92	152	223	25.49	128	200	30.19
104	173	31.02	148	217	26.96	131	201	27.70	109	180	29.89	153	224	25.35	129	201	28.93
105	174	31.35	149	218	27.04	132	202	26.78	110	181	29.50	154	225	25.09	130	202	27.70
106	175	31.09	150	219	26.88	133	203	26.22	111	182	29.25	155	226	25.03	131	203	26.17
107	176	30.87	151	220	26.84	134	204	25.69	112	183	28.62	156	227	24.59	132	204	25.03
108	177	30.40	152	221	26.50	135	205	25.39	113	184	28.23	157	228	24.50	133	205	24.44
109	178	30.17	153	222	26.38	136	206	25.16	114	185	28.00	158	229	23.95	134	206	23.93
110	179	30.01	154	223	26.05	137	207	25.26	115	186	27.90	159	230	23.94	135	207	23.53
111	180	29.54	155	224	25.93	138	208	25.20	116	187	27.68	160	231	23.60	136	208	23.12
112	181	29.04	156	225	25.57	139	209	25.55	117	188	28.00	161	232	23.60	137	209	23.08
113	182	29.03	157	226	25.41	140	210	25.29	118	189	28.26	162	233	23.37	138	210	22.90
114	183	29.02	158	227	24.78	141	211	25.67	119	190	28.44	163	234	23.18	139	211	23.31
115	184	29.05	159	228	24.64	142	212	25.67	120	191	29.43	164	235	22.44	140	212	23.25
116	185	29.16	160	229	24.19	143	213	25.77	121	192	29.91	165	236	22.02	141	213	23.71
117	186	29.34	161	230	24.02	144	214	25.88	122	193	30.09	166	237	21.35	142	214	23.71
118	187	29.55	**$Z = 70$ (Yb)**			145	215	25.93	123	194	30.82	**$Z = 72$ (Hf)**			143	215	24.22
			101	171	28.60							99	171	24.26			

TABLE I. (*Continued*)

N	A	$B_{\rm f}$ (MeV)	N	A	$B_{\rm f}$ (MeV)	N	A	$B_{\rm f}$ (MeV)	N	A	$B_{\rm f}$ (MeV)	N	A	$B_{\rm f}$ (MeV)	N	A	$B_{\rm f}$ (MeV)
$Z = 72$ (Hf)			**$Z = 73$ (Ta)**			**$Z = 73$ (Ta)**			**$Z = 74$ (W)**			**$Z = 74$ (W)**			**$Z = 75$ (Re)**		
144	216	24.07	116	189	26.66	160	233	22.53	129	203	28.08	173	247	18.59	138	213	21.62
145	217	24.25	117	190	26.91	161	234	22.59	130	204	26.83	**$Z = 75$ (Re)**			139	214	21.68
146	218	24.23	118	191	27.09	162	235	22.46	131	205	25.26	96	171	17.51	140	215	21.18
147	219	24.43	119	192	27.48	163	236	22.27	132	206	24.09	97	172	17.94	141	216	21.37
148	220	24.29	120	193	27.79	164	237	21.91	133	207	23.14	98	173	18.13	142	217	21.09
149	221	24.49	121	194	28.70	165	238	21.55	134	208	22.79	99	174	18.81	143	218	21.36
150	222	24.41	122	195	29.03	166	239	20.94	135	209	22.42	100	175	19.23	144	219	21.33
151	223	24.46	123	196	29.80	167	240	20.77	136	210	21.83	101	176	19.95	145	220	21.43
152	224	24.44	124	197	30.19	168	241	20.12	137	211	21.95	102	177	20.56	146	221	21.74
153	225	24.30	125	198	31.07	169	242	19.95	138	212	21.77	103	178	21.38	147	222	21.91
154	226	24.11	126	199	31.35	170	243	19.48	139	213	21.83	104	179	21.82	148	223	22.00
155	227	24.08	127	200	30.55	**$Z = 74$ (W)**			140	214	21.61	105	180	22.50	149	224	22.00
156	228	23.65	128	201	29.64	97	171	19.82	141	215	22.07	106	181	22.91	150	225	22.06
157	229	23.56	129	202	28.48	98	172	20.03	142	216	22.08	107	182	23.49	151	226	22.09
158	230	23.18	130	203	27.06	99	173	20.71	143	217	22.49	108	183	23.62	152	227	22.11
159	231	23.09	131	204	25.86	100	174	21.16	144	218	22.27	109	184	23.77	153	228	22.13
160	232	22.83	132	205	24.55	101	175	21.80	145	219	22.16	110	185	23.66	154	229	21.68
161	233	22.81	133	206	23.91	102	176	22.25	146	220	22.40	111	186	24.13	155	230	21.65
162	234	22.66	134	207	23.28	103	177	22.97	147	221	22.46	112	187	24.13	156	231	21.35
163	235	22.39	135	208	23.13	104	178	23.47	148	222	22.44	113	188	24.77	157	232	21.47
164	236	22.03	136	209	22.60	105	179	24.14	149	223	22.53	114	189	25.13	158	233	21.12
165	237	21.57	137	210	22.75	106	180	24.57	150	224	22.64	115	190	25.99	159	234	21.24
166	238	20.94	138	211	22.70	107	181	25.13	151	225	22.68	116	191	26.24	160	235	20.93
167	239	20.74	139	212	22.51	108	182	25.26	152	226	22.71	117	192	26.37	161	236	21.05
168	240	20.04	140	213	22.78	109	183	25.58	153	227	22.66	118	193	26.57	162	237	21.02
$Z = 73$ (Ta)			141	214	23.19	110	184	25.44	154	228	22.45	119	194	26.64	163	238	20.94
98	171	21.96	142	215	23.24	111	185	25.71	155	229	22.47	120	195	26.76	164	239	20.63
99	172	22.76	143	216	23.69	112	186	25.85	156	230	22.08	121	196	27.44	165	240	20.44
100	173	23.14	144	217	23.46	113	187	26.36	157	231	21.99	122	197	27.93	166	241	19.98
101	174	23.93	145	218	23.65	114	188	26.71	158	232	21.60	123	198	28.69	167	242	19.94
102	175	24.41	146	219	23.71	115	189	26.40	159	233	21.69	124	199	29.07	168	243	19.41
103	176	25.17	147	220	23.92	116	190	26.43	160	234	21.49	125	200	29.91	169	244	19.42
104	177	25.42	148	221	23.78	117	191	26.55	161	235	21.49	126	201	30.22	170	245	19.12
105	178	26.20	149	222	23.90	118	192	26.86	162	236	21.49	127	202	29.48	171	246	19.28
106	179	26.62	150	223	23.90	119	193	27.01	163	237	21.27	128	203	28.54	172	247	18.75
107	180	27.26	151	224	24.02	120	194	27.44	164	238	20.96	129	204	27.39	173	248	18.68
108	181	27.37	152	225	23.98	121	195	27.99	165	239	20.80	130	205	26.18	174	249	18.16
109	182	27.58	153	226	23.94	122	196	28.45	166	240	20.27	131	206	25.13	175	250	17.93
110	183	27.62	154	227	23.69	123	197	29.18	167	241	20.19	132	207	23.73	**$Z = 76$ (Os)**		
111	184	28.00	155	228	23.64	124	198	29.63	168	242	19.66	133	208	22.96	95	171	15.38
112	185	27.79	156	229	23.26	125	199	30.69	169	243	19.56	134	209	22.37	96	172	15.49
113	186	27.72	157	230	23.20	126	200	30.96	170	244	19.17	135	210	22.22	97	173	15.87
114	187	27.14	158	231	22.75	127	201	30.05	171	245	19.23	136	211	21.72	98	174	16.01
115	188	26.84	159	232	22.83	128	202	29.28	172	246	18.74	137	212	21.67	99	175	16.37

TABLE I. (*Continued*)

N	A	$B_{\rm f}$ (MeV)	N	A	$B_{\rm f}$ (MeV)	N	A	$B_{\rm f}$ (MeV)	N	A	$B_{\rm f}$ (MeV)	N	A	$B_{\rm f}$ (MeV)	N	A	$B_{\rm f}$ (MeV)
$Z = 76$ (Os)			**$Z = 76$ (Os)**			**$Z = 77$ (Ir)**			**$Z = 77$ (Ir)**			**$Z = 78$ (Pt)**			**$Z = 78$ (Pt)**		
100	176	16.97	144	220	19.57	103	180	16.65	147	224	18.99	103	181	14.43	147	225	16.98
101	177	17.58	145	221	19.84	104	181	17.26	148	225	19.08	104	182	14.90	148	226	17.08
102	178	18.12	146	222	19.90	105	182	17.82	149	226	19.48	105	183	15.46	149	227	17.55
103	179	18.79	147	223	20.25	106	183	18.30	150	227	19.49	106	184	16.09	150	228	17.45
104	180	19.49	148	224	20.41	107	184	18.84	151	228	19.83	107	185	16.66	151	229	17.75
105	181	20.17	149	225	20.50	108	185	18.98	152	229	19.46	108	186	17.06	152	230	17.65
106	182	20.76	150	226	20.66	109	186	19.53	153	230	19.44	109	187	17.59	153	231	17.33
107	183	21.20	151	227	20.67	110	187	19.59	154	231	18.76	110	188	17.75	154	232	17.22
108	184	21.29	152	228	20.66	111	188	20.06	155	232	18.97	111	189	18.26	155	233	17.47
109	185	21.41	153	229	20.39	112	189	20.15	156	233	18.88	112	190	18.80	156	234	17.42
110	186	21.44	154	230	19.94	113	190	20.69	157	234	19.17	113	191	19.60	157	235	17.54
111	187	21.67	155	231	19.94	114	191	20.94	158	235	18.79	114	192	20.08	158	236	17.24
112	188	21.75	156	232	19.79	115	192	22.19	159	236	18.67	115	193	20.84	159	237	17.18
113	189	22.38	157	233	20.14	116	193	23.18	160	237	18.67	116	194	21.47	160	238	17.33
114	190	22.89	158	234	19.80	117	194	23.84	161	238	18.93	117	195	22.26	161	239	17.49
115	191	23.85	159	235	19.70	118	195	24.31	162	239	19.09	118	196	23.01	162	240	17.63
116	192	24.84	160	236	19.62	119	196	24.95	163	240	18.93	119	197	23.67	163	241	17.56
117	193	25.33	161	237	19.79	120	197	25.27	164	241	18.49	120	198	24.54	164	242	17.18
118	194	25.58	162	238	19.97	121	198	26.22	165	242	18.42	121	199	25.52	165	243	16.97
119	195	25.84	163	239	19.78	122	199	26.92	166	243	17.94	122	200	26.30	166	244	16.82
120	196	26.15	164	240	19.21	123	200	27.70	167	244	18.12	123	201	27.06	167	245	16.80
121	197	26.75	165	241	19.22	124	201	28.18	168	245	18.04	124	202	27.51	168	246	16.70
122	198	27.29	166	242	18.75	125	202	29.05	169	246	18.16	125	203	28.34	169	247	17.00
123	199	28.07	167	243	18.78	126	203	29.35	170	247	17.94	126	204	28.50	170	248	16.86
124	200	28.54	168	244	18.53	127	204	28.46	171	248	18.50	127	205	27.64	171	249	17.30
125	201	29.55	169	245	18.61	128	205	27.77	172	249	18.17	128	206	26.98	172	250	17.33
126	202	29.83	170	246	18.47	129	206	26.69	173	250	18.03	129	207	25.77	173	251	17.54
127	203	29.07	171	247	18.68	130	207	25.59	174	251	17.57	130	208	24.77	174	252	17.33
128	204	28.21	172	248	18.28	131	208	24.27	175	252	17.73	131	209	23.44	175	253	17.54
129	205	27.08	173	249	18.17	132	209	22.95	176	253	17.45	132	210	22.33	176	254	17.49
130	206	25.98	174	250	17.78	133	210	21.98	177	254	18.25	133	211	21.48	177	255	17.77
131	207	24.67	175	251	17.26	134	211	21.45	178	255	18.03	134	212	20.81	178	256	17.75
132	208	23.29	176	252	17.37	135	212	21.13	179	256	18.17	135	213	20.32	179	257	17.89
133	209	22.24	177	253	18.11	136	213	20.75	**$Z = 78$ (Pt)**			136	214	19.74	180	258	17.65
134	210	21.74	**$Z = 77$ (Ir)**			137	214	20.50	93	171	11.36	137	215	19.44	181	259	17.70
135	211	21.53	94	171	13.83	138	215	19.99	94	172	11.73	138	216	18.97	182	260	17.33
136	212	21.04	95	172	14.18	139	216	19.49	95	173	12.23	139	217	18.35	**$Z = 79$ (Au)**		
137	213	20.80	96	173	13.98	140	217	18.91	96	174	12.39	140	218	17.75	92	171	10.83
138	214	20.46	97	174	14.11	141	218	18.58	97	175	12.52	141	219	17.32	93	172	10.94
139	215	20.41	98	175	14.14	142	219	18.31	98	176	12.38	142	220	16.90	94	173	10.94
140	216	20.12	99	176	14.66	143	220	18.46	99	177	12.48	143	221	16.70	95	174	10.64
141	217	19.75	100	177	14.77	144	221	18.27	100	178	12.82	144	222	16.67	96	175	11.00
142	218	19.50	101	178	15.47	145	222	18.57	101	179	13.34	145	223	16.70	97	176	11.28
143	219	19.57	102	179	16.03	146	223	18.62	102	180	13.78	146	224	16.78	98	177	11.07

TABLE I. (*Continued*)

N	A	$B_{\rm f}$ (MeV)	N	A	$B_{\rm f}$ (MeV)	N	A	$B_{\rm f}$ (MeV)	N	A	$B_{\rm f}$ (MeV)	N	A	$B_{\rm f}$ (MeV)	N	A	$B_{\rm f}$ (MeV)
$Z = 79$ (Au)			**$Z = 79$ (Au)**			**$Z = 80$ (Hg)**			**$Z = 80$ (Hg)**			**$Z = 80$ (Hg)**			**$Z = 81$ (Tl)**		
99	178	11.23	143	222	15.58	92	172	9.81	136	216	18.33	180	260	17.79	128	209	24.72
100	179	11.36	144	223	15.51	93	173	9.79	137	217	17.73	181	261	17.84	129	210	23.55
101	180	11.83	145	224	15.44	94	174	9.63	138	218	17.04	182	262	17.69	130	211	22.42
102	181	12.28	146	225	15.35	95	175	9.77	139	219	16.53	183	263	17.75	131	212	21.58
103	182	12.76	147	226	15.71	96	176	9.62	140	220	15.69	184	264	17.41	132	213	20.79
104	183	13.20	148	227	15.79	97	177	9.41	141	221	15.13	185	265	16.52	133	214	19.97
105	184	13.84	149	228	16.52	98	178	9.32	142	222	14.56	186	266	15.63	134	215	19.19
106	185	14.31	150	229	16.18	99	179	9.68	143	223	14.41	**$Z = 81$ (Tl)**			135	216	18.50
107	186	15.03	151	230	16.98	100	180	9.81	144	224	14.13	92	173	9.11	136	217	17.78
108	187	15.33	152	231	16.31	101	181	10.27	145	225	14.19	93	174	8.96	137	218	17.31
109	188	16.01	153	232	16.48	102	182	10.85	146	226	14.30	94	175	9.13	138	219	16.50
110	189	16.57	154	233	16.25	103	183	11.32	147	227	14.59	95	176	9.19	139	220	15.88
111	190	17.16	155	234	16.50	104	184	11.92	148	228	14.71	96	177	9.04	140	221	14.99
112	191	17.99	156	235	16.36	105	185	12.43	149	229	15.09	97	178	9.01	141	222	14.33
113	192	18.87	157	236	16.46	106	186	12.99	150	230	14.95	98	179	8.81	142	223	13.64
114	193	19.26	158	237	16.23	107	187	13.50	151	231	15.16	99	180	8.65	143	224	13.49
115	194	19.96	159	238	16.41	108	188	13.98	152	232	14.97	100	181	8.86	144	225	13.33
116	195	20.54	160	239	16.47	109	189	14.52	153	233	15.11	101	182	8.98	145	226	13.54
117	196	21.47	161	240	16.58	110	190	15.22	154	234	14.85	102	183	9.49	146	227	13.53
118	197	22.31	162	241	16.63	111	191	16.02	155	235	15.09	103	184	9.87	147	228	13.89
119	198	23.16	163	242	16.61	112	192	16.75	156	236	14.97	104	185	10.44	148	229	13.86
120	199	23.97	164	243	16.24	113	193	17.56	157	237	14.99	105	186	10.97	149	230	14.15
121	200	25.07	165	244	16.08	114	194	18.10	158	238	14.91	106	187	11.48	150	231	13.99
122	201	25.78	166	245	15.69	115	195	18.79	159	239	14.90	107	188	12.11	151	232	14.20
123	202	26.53	167	246	15.99	116	196	19.65	160	240	14.97	108	189	12.74	152	233	13.96
124	203	27.01	168	247	16.24	117	197	20.48	161	241	15.21	109	190	13.49	153	234	14.09
125	204	27.95	169	248	16.77	118	198	21.45	162	242	15.24	110	191	14.31	154	235	13.81
126	205	28.03	170	249	16.94	119	199	22.24	163	243	15.22	111	192	15.13	155	236	13.94
127	206	27.09	171	250	17.57	120	200	23.23	164	244	14.90	112	193	15.99	156	237	13.78
128	207	26.36	172	251	17.57	121	201	24.05	165	245	14.71	113	194	16.38	157	238	14.12
129	208	25.36	173	252	17.82	122	202	24.79	166	246	15.11	114	195	17.08	158	239	14.02
130	209	24.25	174	253	17.39	123	203	25.55	167	247	15.50	115	196	18.04	159	240	14.29
131	210	22.93	175	254	17.70	124	204	26.11	168	248	15.77	116	197	18.85	160	241	14.07
132	211	21.87	176	255	17.77	125	205	27.09	169	249	16.12	117	198	19.73	161	242	14.31
133	212	21.29	177	256	17.64	126	206	27.21	170	250	16.40	118	199	20.63	162	243	14.37
134	213	20.54	178	257	17.61	127	207	26.10	171	251	16.79	119	200	21.66	163	244	14.43
135	214	19.95	179	258	17.86	128	208	25.51	172	252	16.89	120	201	22.23	164	245	14.19
136	215	19.25	180	259	17.60	129	209	24.37	173	253	17.28	121	202	23.29	165	246	14.35
137	216	18.84	181	260	17.61	130	210	23.32	174	254	17.38	122	203	24.04	166	247	14.53
138	217	18.24	182	261	17.31	131	211	22.17	175	255	17.74	123	204	24.80	167	248	14.88
139	218	17.77	183	262	17.32	132	212	21.27	176	256	17.62	124	205	25.49	168	249	15.23
140	219	16.95	184	263	17.27	133	213	20.44	177	257	17.77	125	206	26.38	169	250	15.62
141	220	16.41	**$Z = 80$ (Hg)**			134	214	19.80	178	258	17.76	126	207	26.50	170	251	15.98
142	221	15.77	91	171	10.03	135	215	19.00	179	259	18.02	127	208	25.55	171	252	16.53

TABLE I. (*Continued*)

N	A	$B_{\rm f}$ (MeV)	N	A	$B_{\rm f}$ (MeV)	N	A	$B_{\rm f}$ (MeV)	N	A	$B_{\rm f}$ (MeV)	N	A	$B_{\rm f}$ (MeV)	N	A	$B_{\rm f}$ (MeV)
$Z = 81$ (Tl)			**$Z = 82$ (Pb)**			**$Z = 82$ (Pb)**			**$Z = 83$ (Bi)**			**$Z = 83$ (Bi)**			**$Z = 84$ (Po)**		
172	253	16.75	119	201	19.67	163	245	13.21	109	192	9.99	153	236	11.56	99	183	4.89
173	254	17.20	120	202	20.48	164	246	13.24	110	193	10.59	154	237	11.36	100	184	5.49
174	255	17.10	121	203	20.91	165	247	13.42	111	194	11.14	155	238	11.14	101	185	5.93
175	256	17.50	122	204	21.91	166	248	13.60	112	195	11.79	156	239	10.96	102	186	6.35
176	257	17.58	123	205	23.08	167	249	13.85	113	196	12.31	157	240	11.28	103	187	6.64
177	258	17.76	124	206	23.94	168	250	14.06	114	197	13.29	158	241	11.29	104	188	6.92
178	259	17.90	125	207	24.76	169	251	14.61	115	198	14.23	159	242	11.55	105	189	7.27
179	260	18.33	126	208	24.95	170	252	14.85	116	199	15.22	160	243	11.44	106	190	7.55
180	261	18.18	127	209	23.97	171	253	15.29	117	200	16.18	161	244	11.68	107	191	7.89
181	262	18.51	128	210	22.91	172	254	15.28	118	201	16.99	162	245	11.72	108	192	8.25
182	263	18.25	129	211	21.88	173	255	15.72	119	202	17.90	163	246	12.08	109	193	8.66
183	264	18.37	130	212	20.77	174	256	15.67	120	203	18.71	164	247	11.97	110	194	9.46
184	265	17.79	131	213	19.87	175	257	16.18	121	204	19.59	165	248	12.66	111	195	9.59
185	266	16.95	132	214	19.13	176	258	16.30	122	205	20.47	166	249	12.78	112	196	10.29
186	267	15.93	133	215	18.43	177	259	17.03	123	206	21.42	167	250	13.10	113	197	10.66
187	268	14.45	134	216	17.95	178	260	17.33	124	207	22.28	168	251	13.46	114	198	11.52
188	269	13.28	135	217	17.48	179	261	17.87	125	208	23.23	169	252	14.06	115	199	12.37
$Z = 82$ (Pb)			136	218	16.83	180	262	17.97	126	209	23.88	170	253	14.25	116	200	13.31
93	175	7.62	137	219	16.13	181	263	18.30	127	210	22.74	171	254	14.59	117	201	14.18
94	176	7.58	138	220	15.33	182	264	18.08	128	211	21.76	172	255	14.74	118	202	15.14
95	177	7.74	139	221	14.45	183	265	18.20	129	212	20.49	173	256	14.94	119	203	16.15
96	178	7.99	140	222	13.70	184	266	17.71	130	213	19.17	174	257	14.81	120	204	17.02
97	179	8.15	141	223	12.89	185	267	16.50	131	214	17.89	175	258	15.42	121	205	18.08
98	180	8.47	142	224	12.48	186	268	15.43	132	215	16.79	176	259	15.81	122	206	19.02
99	181	8.48	143	225	12.43	187	269	13.94	133	216	16.05	177	260	16.27	123	207	20.01
100	182	8.63	144	226	12.34	188	270	12.96	134	217	15.65	178	261	16.42	124	208	20.81
101	183	8.65	145	227	12.30	189	271	12.57	135	218	15.16	179	262	17.06	125	209	22.24
102	184	8.92	146	228	12.16	190	272	12.09	136	219	14.45	180	263	17.19	126	210	22.14
103	185	9.12	147	229	12.39	191	273	11.96	137	220	14.02	181	264	17.59	127	211	21.33
104	186	9.61	148	230	12.58	**$Z = 83$ (Bi)**			138	221	13.33	182	265	17.41	128	212	20.27
105	187	9.83	149	231	12.82	95	178	5.33	139	222	12.58	183	266	17.52	129	213	18.99
106	188	10.32	150	232	12.67	96	179	5.40	140	223	12.26	184	267	16.96	130	214	17.76
107	189	10.63	151	233	12.90	97	180	5.69	141	224	12.31	185	268	15.81	131	215	16.47
108	190	11.18	152	234	12.64	98	181	5.73	142	225	12.14	186	269	14.74	132	216	15.42
109	191	11.68	153	235	12.70	99	182	6.40	143	226	11.92	187	270	13.30	133	217	14.56
110	192	12.85	154	236	12.41	100	183	6.53	144	227	11.79	188	271	11.66	134	218	13.85
111	193	13.57	155	237	12.40	101	184	7.16	145	228	11.71	189	272	11.88	135	219	12.93
112	194	14.50	156	238	12.23	102	185	7.38	146	229	11.66	190	273	11.25	136	220	12.47
113	195	14.77	157	239	12.37	103	186	7.75	147	230	11.77	191	274	11.23	137	221	12.31
114	196	15.66	158	240	12.42	104	187	7.75	148	231	11.44	192	275	10.76	138	222	11.91
115	197	16.36	159	241	12.81	105	188	8.14	149	232	11.84	193	276	9.86	139	223	11.70
116	198	17.28	160	242	12.77	106	189	8.60	150	233	11.65	**$Z = 84$ (Po)**			140	224	11.46
117	199	18.09	161	243	13.01	107	190	9.15	151	234	11.87	97	181	3.89	141	225	11.24
118	200	18.89	162	244	13.07	108	191	9.45	152	235	11.56	98	182	4.35	142	226	10.98

TABLE I. (*Continued*)

N	A	$B_{\rm f}$ (MeV)	N	A	$B_{\rm f}$ (MeV)	N	A	$B_{\rm f}$ (MeV)	N	A	$B_{\rm f}$ (MeV)	N	A	$B_{\rm f}$ (MeV)	N	A	$B_{\rm f}$ (MeV)
$Z = 84$ (Po)			**$Z = 84$ (Po)**			**$Z = 85$ (At)**			**$Z = 85$ (At)**			**$Z = 86$ (Rn)**			**$Z = 86$ (Rn)**		
143	227	10.92	187	271	12.36	133	218	13.31	177	262	14.18	122	208	15.94	166	252	9.52
144	228	10.68	188	272	11.82	134	219	12.46	178	263	14.37	123	209	16.75	167	253	9.81
145	229	10.66	189	273	11.49	135	220	12.12	179	264	14.66	124	210	17.61	168	254	10.03
146	230	10.63	190	274	10.85	136	221	11.75	180	265	14.81	125	211	18.47	169	255	10.52
147	231	10.75	191	275	10.84	137	222	11.64	181	266	15.21	126	212	18.63	170	256	10.81
148	232	10.69	192	276	10.02	138	223	11.13	182	267	15.13	127	213	17.65	171	257	11.22
149	233	10.97	193	277	9.16	139	224	11.03	183	268	15.30	128	214	16.69	172	258	11.60
150	234	10.76	194	278	8.48	140	225	10.74	184	269	14.82	129	215	15.45	173	259	11.32
151	235	11.08	195	279	7.86	141	226	10.42	185	270	13.70	130	216	14.24	174	260	11.35
152	236	10.83	**$Z = 85$ (At)**			142	227	10.11	186	271	12.88	131	217	13.52	175	261	11.91
153	237	10.85	99	184	4.12	143	228	10.02	187	272	11.34	132	218	12.83	176	262	12.30
154	238	10.49	100	185	4.39	144	229	9.83	188	273	10.89	133	219	12.02	177	263	12.79
155	239	10.49	101	186	4.68	145	230	9.86	189	274	10.46	134	220	11.47	178	264	12.99
156	240	10.11	102	187	5.00	146	231	9.78	190	275	10.14	135	221	11.18	179	265	13.42
157	241	10.28	103	188	5.44	147	232	9.97	191	276	10.05	136	222	10.82	180	266	13.55
158	242	10.34	104	189	5.56	148	233	9.93	192	277	9.12	137	223	10.57	181	267	13.74
159	243	10.62	105	190	5.94	149	234	10.18	193	278	8.69	138	224	10.30	182	268	13.81
160	244	10.61	106	191	6.02	150	235	10.36	194	279	7.97	139	225	9.72	183	269	14.07
161	245	10.99	107	192	6.76	151	236	10.60	195	280	7.13	140	226	9.45	184	270	13.59
162	246	10.95	108	193	7.24	152	237	10.53	196	281	6.46	141	227	9.26	185	271	12.54
163	247	11.42	109	194	7.67	153	238	10.31	197	282	6.20	142	228	9.04	186	272	11.68
164	248	11.35	110	195	7.96	154	239	10.04	**$Z = 86$ (Rn)**			143	229	8.88	187	273	10.71
165	249	11.56	111	196	8.33	155	240	9.79	100	186	4.19	144	230	8.81	188	274	10.02
166	250	11.69	112	197	8.63	156	241	9.58	101	187	4.43	145	231	8.81	189	275	9.74
167	251	12.04	113	198	9.10	157	242	9.94	102	188	4.45	146	232	8.82	190	276	9.42
168	252	12.29	114	199	9.95	158	243	9.73	103	189	4.62	147	233	8.87	191	277	9.22
169	253	12.83	115	200	10.80	159	244	10.19	104	190	4.54	148	234	8.92	192	278	8.45
170	254	12.98	116	201	11.73	160	245	10.17	105	191	4.49	149	235	9.21	193	279	8.04
171	255	13.35	117	202	12.66	161	246	10.41	106	192	4.63	150	236	9.38	194	280	7.37
172	256	13.73	118	203	13.70	162	247	10.42	107	193	5.02	151	237	9.76	195	281	6.62
173	257	13.69	119	204	14.72	163	248	10.60	108	194	5.43	152	238	9.70	196	282	6.09
174	258	13.70	120	205	15.41	164	249	10.49	109	195	6.05	153	239	9.73	197	283	5.45
175	259	14.20	121	206	16.63	165	250	10.75	110	196	6.41	154	240	9.30	198	284	5.13
176	260	14.61	122	207	17.46	166	251	10.88	111	197	6.83	155	241	9.17	199	285	4.43
177	261	15.12	123	208	18.31	167	252	11.26	112	198	7.40	156	242	8.98	200	286	4.00
178	262	15.24	124	209	19.10	168	253	11.47	113	199	8.09	157	243	9.26	**$Z = 87$ (Fr)**		
179	263	15.83	125	210	19.99	169	254	12.04	114	200	8.61	158	244	9.12	102	189	4.24
180	264	16.02	126	211	20.27	170	255	12.22	115	201	9.39	159	245	9.01	103	190	4.44
181	265	16.41	127	212	19.37	171	256	12.53	116	202	10.29	160	246	9.02	104	191	4.33
182	266	16.33	128	213	18.56	172	257	13.04	117	203	11.16	161	247	9.28	105	192	4.43
183	267	16.51	129	214	17.35	173	258	12.82	118	204	12.10	162	248	9.34	106	193	4.38
184	268	16.05	130	215	16.03	174	259	12.94	119	205	13.20	163	249	9.51	107	194	4.35
185	269	14.82	131	216	14.99	175	260	13.24	120	206	14.20	164	250	9.40	108	195	4.48
186	270	13.86	132	217	14.16	176	261	13.65	121	207	15.14	165	251	9.41	109	196	4.58

TABLE I. (*Continued*)

N	A	$B_{\rm f}$ (MeV)	N	A	$B_{\rm f}$ (MeV)	N	A	$B_{\rm f}$ (MeV)	N	A	$B_{\rm f}$ (MeV)	N	A	$B_{\rm f}$ (MeV)	N	A	$B_{\rm f}$ (MeV)
$Z = 87$ (Fr)			**$Z = 87$ (Fr)**			**$Z = 87$ (Fr)**			**$Z = 88$ (Ra)**			**$Z = 88$ (Ra)**			**$Z = 89$ (Ac)**		
110	197	5.18	154	241	8.83	198	285	5.05	142	230	7.04	186	274	9.78	130	219	10.03
111	198	5.82	155	242	8.66	199	286	4.53	143	231	7.01	187	275	8.88	131	220	9.71
112	199	6.39	156	243	8.44	200	287	4.01	144	232	6.94	188	276	8.33	132	221	9.34
113	200	7.10	157	244	8.45	201	288	3.85	145	233	6.97	189	277	8.48	133	222	9.13
114	201	7.62	158	245	8.24	202	289	3.27	146	234	6.90	190	278	8.22	134	223	8.69
115	202	8.33	159	246	8.09	**$Z = 88$ (Ra)**			147	235	7.16	191	279	8.20	135	224	8.50
116	203	8.92	160	247	8.12	104	192	3.92	148	236	7.33	192	280	7.64	136	225	8.05
117	204	9.64	161	248	8.42	105	193	3.77	149	237	7.70	193	281	7.16	137	226	7.71
118	205	10.94	162	249	8.44	106	194	3.76	150	238	7.79	194	282	6.46	138	227	7.53
119	206	11.98	163	250	8.66	107	195	3.46	151	239	8.26	195	283	6.10	139	228	7.24
120	207	12.85	164	251	8.59	108	196	3.72	152	240	8.24	196	284	5.56	140	229	6.68
121	208	13.71	165	252	8.53	109	197	4.12	153	241	8.24	197	285	5.19	141	230	6.49
122	209	14.60	166	253	8.53	110	198	3.99	154	242	7.95	198	286	4.77	142	231	6.24
123	210	15.40	167	254	8.83	111	199	4.63	155	243	7.78	199	287	4.26	143	232	6.19
124	211	16.02	168	255	9.00	112	200	5.12	156	244	7.49	200	288	3.78	144	233	6.08
125	212	16.72	169	256	9.56	113	201	5.85	157	245	7.61	201	289	3.39	145	234	6.16
126	213	16.66	170	257	9.79	114	202	6.26	158	246	7.34	202	290	2.91	146	235	6.27
127	214	15.65	171	258	10.05	115	203	6.89	159	247	7.39	203	291	2.63	147	236	6.89
128	215	14.81	172	259	10.40	116	204	7.49	160	248	7.20	204	292	2.24	148	237	7.08
129	216	13.46	173	260	10.44	117	205	8.51	161	249	7.29	**$Z = 89$ (Ac)**			149	238	7.61
130	217	12.74	174	261	10.20	118	206	9.75	162	250	7.21	106	195	3.40	150	239	7.75
131	218	12.40	175	262	10.95	119	207	10.82	163	251	7.26	107	196	3.29	151	240	8.26
132	219	11.57	176	263	11.42	120	208	11.70	164	252	7.08	108	197	3.24	152	241	8.19
133	220	11.33	177	264	11.72	121	209	12.54	165	253	7.14	109	198	3.44	153	242	8.15
134	221	10.81	178	265	11.91	122	210	13.26	166	254	7.10	110	199	3.45	154	243	7.84
135	222	10.47	179	266	12.35	123	211	14.00	167	255	7.33	111	200	3.64	155	244	7.62
136	223	10.02	180	267	12.32	124	212	14.40	168	256	7.48	112	201	4.05	156	245	7.35
137	224	9.64	181	268	12.65	125	213	15.11	169	257	7.75	113	202	4.81	157	246	7.36
138	225	9.22	182	269	12.79	126	214	14.94	170	258	8.07	114	203	5.19	158	247	7.12
139	226	9.02	183	270	13.05	127	215	13.93	171	259	8.52	115	204	5.72	159	248	7.10
140	227	8.61	184	271	12.54	128	216	13.01	172	260	9.00	116	205	6.49	160	249	6.86
141	228	8.36	185	272	11.55	129	217	11.80	173	261	8.87	117	206	7.42	161	250	6.94
142	229	8.12	186	273	10.76	130	218	11.25	174	262	9.03	118	207	8.46	162	251	6.74
143	230	8.04	187	274	9.74	131	219	10.81	175	263	9.73	119	208	9.50	163	252	6.81
144	231	7.96	188	275	9.09	132	220	10.25	176	264	10.16	120	209	10.58	164	253	6.59
145	232	8.01	189	276	9.18	133	221	10.03	177	265	10.73	121	210	11.31	165	254	6.50
146	233	7.92	190	277	8.93	134	222	9.57	178	266	10.80	122	211	12.03	166	255	6.27
147	234	8.09	191	278	8.72	135	223	9.20	179	267	11.18	123	212	12.65	167	256	6.64
148	235	8.15	192	279	8.17	136	224	8.78	180	268	11.15	124	213	12.99	168	257	6.91
149	236	8.50	193	280	7.72	137	225	8.40	181	269	11.68	125	214	13.52	169	258	7.31
150	237	8.71	194	281	7.03	138	226	8.23	182	270	11.74	126	215	13.36	170	259	7.48
151	238	8.96	195	282	6.58	139	227	8.02	183	271	12.02	127	216	12.19	171	260	7.85
152	239	9.03	196	283	6.14	140	228	7.61	184	272	11.58	128	217	11.08	172	261	8.01
153	240	9.07	197	284	5.60	141	229	7.31	185	273	10.53	129	218	10.40	173	262	7.97

TABLE I. (*Continued*)

N	A	$B_{\rm f}$ (MeV)	N	A	$B_{\rm f}$ (MeV)	N	A	$B_{\rm f}$ (MeV)	N	A	$B_{\rm f}$ (MeV)	N	A	$B_{\rm f}$ (MeV)	N	A	$B_{\rm f}$ (MeV)
$Z = 89$ (Ac)			**$Z = 90$ (Th)**			**$Z = 90$ (Th)**			**$Z = 90$ (Th)**			**$Z = 91$ (Pa)**			**$Z = 91$ (Pa)**		
174	263	8.11	118	208	7.57	162	252	6.40	206	296	2.87	148	239	6.72	192	283	6.01
175	264	8.77	119	209	8.55	163	253	6.22	207	297	3.12	149	240	7.27	193	284	6.11
176	265	9.20	120	210	9.39	164	254	6.07	208	298	3.17	150	241	7.43	194	285	5.93
177	266	9.78	121	211	10.11	165	255	5.86	209	299	3.03	151	242	7.87	195	286	5.85
178	267	9.77	122	212	10.66	166	256	5.53	**$Z = 91$ (Pa)**			152	243	7.79	196	287	5.46
179	268	10.24	123	213	11.34	167	257	5.88	109	200	2.18	153	244	7.76	197	288	5.23
180	269	10.27	124	214	11.68	168	258	6.08	110	201	2.08	154	245	7.40	198	289	4.76
181	270	10.81	125	215	12.34	169	259	6.39	111	202	2.06	155	246	7.13	199	290	4.30
182	271	10.79	126	216	12.17	170	260	6.61	112	203	2.08	156	247	6.89	200	291	3.85
183	272	11.06	127	217	11.02	171	261	7.05	113	204	2.64	157	248	6.91	201	292	3.60
184	273	10.58	128	218	9.99	172	262	7.04	114	205	3.04	158	249	6.66	202	293	3.11
185	274	9.60	129	219	9.17	173	263	6.88	115	206	4.01	159	250	6.67	203	294	2.98
186	275	8.99	130	220	8.45	174	264	7.01	116	207	4.74	160	251	6.34	204	295	2.83
187	276	8.10	131	221	8.27	175	265	7.60	117	208	5.62	161	252	6.35	205	296	2.99
188	277	7.55	132	222	7.99	176	266	8.00	118	209	6.55	162	253	6.05	206	297	3.07
189	278	7.79	133	223	8.20	177	267	8.52	119	210	7.44	163	254	5.87	207	298	3.34
190	279	7.60	134	224	7.85	178	268	8.73	120	211	8.19	164	255	5.58	208	299	3.32
191	280	7.64	135	225	7.59	179	269	9.33	121	212	8.97	165	256	5.35	209	300	3.39
192	281	7.23	136	226	7.20	180	270	9.38	122	213	9.33	166	257	5.17	210	301	3.17
193	282	6.84	137	227	6.98	181	271	9.84	123	214	9.97	167	258	5.30	211	302	3.06
194	283	6.29	138	228	6.52	182	272	9.87	124	215	10.35	168	259	5.42	**$Z = 92$ (U)**		
195	284	5.97	139	229	6.06	183	273	10.09	125	216	10.93	169	260	5.64	111	203	1.21
196	285	5.56	140	230	5.66	184	274	9.65	126	217	10.81	170	261	5.84	112	204	1.14
197	286	5.30	141	231	5.55	185	275	8.66	127	218	9.68	171	262	6.24	113	205	1.74
198	287	4.86	142	232	5.44	186	276	8.08	128	219	8.60	172	263	6.24	114	206	2.27
199	288	4.39	143	233	5.47	187	277	7.27	129	220	8.20	173	264	6.30	115	207	3.24
200	289	3.81	144	234	5.38	188	278	6.84	130	221	7.55	174	265	6.33	116	208	3.84
201	290	3.41	145	235	5.80	189	279	7.06	131	222	6.93	175	266	6.82	117	209	4.59
202	291	3.00	146	236	6.04	190	280	6.90	132	223	6.91	176	267	7.14	118	210	5.44
203	292	2.82	147	237	6.64	191	281	6.97	133	224	7.03	177	268	7.59	119	211	6.51
204	293	2.51	148	238	6.84	192	282	6.66	134	225	6.84	178	269	7.93	120	212	7.18
205	294	2.65	149	239	7.35	193	283	6.31	135	226	6.91	179	270	8.46	121	213	7.85
206	295	2.70	150	240	7.53	194	284	5.87	136	227	6.51	180	271	8.49	122	214	8.30
$Z = 90$ (Th)			151	241	8.00	195	285	5.76	137	228	6.26	181	272	8.98	123	215	8.82
108	198	2.53	152	242	7.97	196	286	5.40	138	229	5.59	182	273	8.91	124	216	9.25
109	199	2.77	153	243	7.89	197	287	5.14	139	230	5.28	183	274	9.13	125	217	9.78
110	200	2.69	154	244	7.61	198	288	4.74	140	231	4.99	184	275	8.65	126	218	9.67
111	201	2.89	155	245	7.36	199	289	4.22	141	232	4.97	185	276	7.57	127	219	8.54
112	202	2.86	156	246	6.94	200	290	3.62	142	233	4.99	186	277	7.09	128	220	7.62
113	203	3.61	157	247	7.12	201	291	3.33	143	234	5.13	187	278	6.41	129	221	7.06
114	204	3.85	158	248	6.88	202	292	3.05	144	235	5.33	188	279	6.23	130	222	6.46
115	205	4.79	159	249	6.72	203	293	2.91	145	236	5.76	189	280	6.35	131	223	5.87
116	206	5.44	160	250	6.59	204	294	2.67	146	237	5.99	190	281	6.20	132	224	5.65
117	207	6.43	161	251	6.63	205	295	2.78	147	238	6.57	191	282	6.31	133	225	5.81

TABLE I. (*Continued*)

N	A	$B_{\rm f}$ (MeV)	N	A	$B_{\rm f}$ (MeV)	N	A	$B_{\rm f}$ (MeV)	N	A	$B_{\rm f}$ (MeV)	N	A	$B_{\rm f}$ (MeV)	N	A	$B_{\rm f}$ (MeV)
$Z = 92$ (U)			**$Z = 92$ (U)**			**$Z = 93$ (Np)**			**$Z = 93$ (Np)**			**$Z = 93$ (Np)**			**$Z = 94$ (Pu)**		
134	226	5.59	178	270	7.09	120	213	6.09	164	257	4.58	208	301	3.40	150	244	6.59
135	227	5.48	179	271	7.58	121	214	6.67	165	258	4.27	209	302	3.48	151	245	6.93
136	228	5.13	180	272	7.64	122	215	7.00	166	259	4.06	210	303	3.50	152	246	7.07
137	229	4.94	181	273	8.06	123	216	7.52	167	260	4.04	211	304	3.66	153	247	7.12
138	230	4.28	182	274	8.06	124	217	7.83	168	261	4.04	212	305	3.65	154	248	6.80
139	231	4.46	183	275	8.26	125	218	8.28	169	262	4.18	213	306	3.85	155	249	6.59
140	232	4.72	184	276	7.72	126	219	8.26	170	263	4.17	214	307	3.83	156	250	6.17
141	233	4.79	185	277	6.71	127	220	7.32	171	264	4.76	215	308	4.08	157	251	5.94
142	234	4.89	186	278	6.26	128	221	6.47	172	265	5.12	**$Z = 94$ (Pu)**			158	252	5.63
143	235	4.87	187	279	5.64	129	222	6.01	173	266	5.23	115	209	1.72	159	253	5.64
144	236	5.03	188	280	5.51	130	223	5.28	174	267	5.29	116	210	2.25	160	254	5.41
145	237	5.43	189	281	5.59	131	224	4.96	175	268	5.78	117	211	3.05	161	255	5.40
146	238	5.63	190	282	5.50	132	225	4.43	176	269	6.18	118	212	3.59	162	256	5.14
147	239	6.21	191	283	5.59	133	226	4.17	177	270	6.60	119	213	4.39	163	257	4.83
148	240	6.38	192	284	5.41	134	227	3.78	178	271	6.51	120	214	5.09	164	258	4.27
149	241	6.93	193	285	5.63	135	228	3.70	179	272	6.68	121	215	5.70	165	259	4.04
150	242	7.10	194	286	5.69	136	229	3.81	180	273	6.56	122	216	6.01	166	260	3.96
151	243	7.50	195	287	5.50	137	230	3.81	181	274	7.01	123	217	6.45	167	261	4.09
152	244	7.46	196	288	5.09	138	231	3.81	182	275	6.93	124	218	6.78	168	262	3.94
153	245	7.39	197	289	4.86	139	232	4.14	183	276	7.01	125	219	7.28	169	263	4.10
154	246	7.21	198	290	4.44	140	233	4.37	184	277	6.43	126	220	7.34	170	264	3.91
155	247	7.03	199	291	4.28	141	234	4.63	185	278	5.72	127	221	6.44	171	265	4.24
156	248	6.64	200	292	3.93	142	235	4.83	186	279	5.19	128	222	5.62	172	266	4.59
157	249	6.57	201	293	3.84	143	236	4.81	187	280	5.08	129	223	5.07	173	267	4.63
158	250	6.31	202	294	3.33	144	237	4.94	188	281	4.79	130	224	4.47	174	268	4.70
159	251	6.37	203	295	3.12	145	238	5.36	189	282	5.00	131	225	4.24	175	269	5.27
160	252	6.04	204	296	2.95	146	239	5.57	190	283	4.90	132	226	3.74	176	270	5.74
161	253	6.00	205	297	3.02	147	240	6.01	191	284	5.12	133	227	3.43	177	271	6.21
162	254	5.74	206	298	3.16	148	241	6.15	192	285	5.11	134	228	2.93	178	272	6.18
163	255	5.48	207	299	3.40	149	242	6.76	193	286	5.37	135	229	2.95	179	273	6.32
164	256	5.02	208	300	3.38	150	243	6.87	194	287	5.26	136	230	3.07	180	274	6.20
165	257	4.78	209	301	3.33	151	244	7.35	195	288	5.43	137	231	3.05	181	275	6.35
166	258	4.61	210	302	3.20	152	245	7.27	196	289	4.96	138	232	3.23	182	276	6.15
167	259	4.64	211	303	3.24	153	246	7.39	197	290	4.73	139	233	3.50	183	277	6.07
168	260	4.70	212	304	3.23	154	247	7.09	198	291	4.52	140	234	3.83	184	278	5.72
169	261	4.89	213	305	3.44	155	248	6.89	199	292	4.34	141	235	4.09	185	279	4.96
170	262	4.95	**$Z = 93$ (Np)**			156	249	6.46	200	293	4.09	142	236	4.49	186	280	4.43
171	263	5.33	113	206	1.16	157	250	6.35	201	294	3.93	143	237	5.00	187	281	4.12
172	264	5.59	114	207	1.66	158	251	6.01	202	295	3.54	144	238	5.26	188	282	4.07
173	265	5.67	115	208	2.52	159	252	5.87	203	296	3.26	145	239	5.74	189	283	4.29
174	266	5.74	116	209	3.05	160	253	5.72	204	297	3.07	146	240	5.98	190	284	4.24
175	267	6.11	117	210	3.72	161	254	5.64	205	298	3.22	147	241	6.35	191	285	4.47
176	268	6.60	118	211	4.49	162	255	5.39	206	299	3.26	148	242	6.41	192	286	4.49
177	269	7.03	119	212	5.21	163	256	5.12	207	300	3.44	149	243	6.66	193	287	4.69

TABLE I. (*Continued*)

N	A	$B_{\rm f}$ (MeV)	N	A	$B_{\rm f}$ (MeV)	N	A	$B_{\rm f}$ (MeV)	N	A	$B_{\rm f}$ (MeV)	N	A	$B_{\rm f}$ (MeV)	N	A	$B_{\rm f}$ (MeV)
$Z = 94$ (Pu)			**$Z = 95$ (Am)**			**$Z = 95$ (Am)**			**$Z = 96$ (Cm)**			**$Z = 96$ (Cm)**			**$Z = 96$ (Cm)**		
194	288	4.59	135	230	2.46	179	274	5.81	120	216	3.31	164	260	4.15	208	304	4.49
195	289	4.73	136	231	2.51	180	275	5.61	121	217	3.78	165	261	4.07	209	305	4.70
196	290	4.65	137	232	2.65	181	276	5.85	122	218	4.09	166	262	3.88	210	306	4.84
197	291	4.68	138	233	2.79	182	277	5.49	123	219	4.59	167	263	3.92	211	307	4.91
198	292	4.47	139	234	3.27	183	278	5.08	124	220	4.99	168	264	3.85	212	308	4.75
199	293	4.32	140	235	3.80	184	279	4.64	125	221	5.62	169	265	4.01	213	309	4.72
200	294	4.03	141	236	4.33	185	280	4.08	126	222	5.64	170	266	3.99	214	310	4.51
201	295	3.84	142	237	4.80	186	281	3.52	127	223	4.85	171	267	4.32	215	311	4.48
202	296	3.51	143	238	5.34	187	282	3.63	128	224	4.16	172	268	4.40	216	312	4.34
203	297	3.34	144	239	5.66	188	283	3.46	129	225	3.69	173	269	4.53	217	313	4.42
204	298	3.04	145	240	6.12	189	284	3.71	130	226	3.02	174	270	4.45	218	314	4.31
205	299	3.18	146	241	6.34	190	285	3.74	131	227	2.68	175	271	4.65	219	315	4.28
206	300	3.28	147	242	6.72	191	286	3.97	132	228	2.11	176	272	4.95	220	316	4.14
207	301	3.58	148	243	6.80	192	287	3.95	133	229	1.99	177	273	5.22	221	317	4.18
208	302	3.69	149	244	6.99	193	288	4.20	134	230	1.87	178	274	5.17	222	318	3.97
209	303	3.89	150	245	6.80	194	289	4.19	135	231	2.00	179	275	5.45	**$Z = 97$ (Bk)**		
210	304	3.96	151	246	6.88	195	290	4.69	136	232	2.10	180	276	5.33	121	218	2.90
211	305	4.15	152	247	6.83	196	291	4.61	137	233	2.24	181	277	5.53	122	219	3.16
212	306	4.22	153	248	6.91	197	292	4.76	138	234	2.61	182	278	5.34	123	220	3.65
213	307	4.40	154	249	6.59	198	293	4.61	139	235	3.23	183	279	5.13	124	221	3.93
214	308	4.34	155	250	6.37	199	294	4.40	140	236	3.81	184	280	4.40	125	222	4.49
215	309	4.36	156	251	5.87	200	295	4.15	141	237	4.34	185	281	3.31	126	223	4.66
216	310	4.12	157	252	5.79	201	296	3.96	142	238	4.92	186	282	2.84	127	224	3.98
217	311	4.20	158	253	5.41	202	297	3.66	143	239	5.48	187	283	2.72	128	225	3.44
218	312	4.10	159	254	5.45	203	298	3.53	144	240	5.85	188	284	2.59	129	226	2.84
$Z = 95$ (Am)			160	255	5.19	204	299	3.34	145	241	6.32	189	285	2.85	130	227	2.17
117	212	2.40	161	256	5.17	205	300	3.60	146	242	6.56	190	286	2.81	131	228	2.17
118	213	3.13	162	257	4.89	206	301	3.69	147	243	6.97	191	287	3.05	132	229	1.93
119	214	3.57	163	258	4.59	207	302	3.99	148	244	6.92	192	288	3.14	133	230	1.72
120	215	4.03	164	259	4.07	208	303	4.11	149	245	7.13	193	289	3.41	134	231	1.64
121	216	4.56	165	260	4.00	209	304	4.33	150	246	7.02	194	290	3.58	135	232	1.81
122	217	4.81	166	261	3.86	210	305	4.43	151	247	7.11	195	291	3.97	136	233	1.94
123	218	5.32	167	262	3.99	211	306	4.62	152	248	6.80	196	292	4.14	137	234	2.27
124	219	5.60	168	263	3.92	212	307	4.64	153	249	6.56	197	293	4.45	138	235	2.71
125	220	6.19	169	264	4.17	213	308	4.66	154	250	6.25	198	294	4.26	139	236	3.37
126	221	6.23	170	265	4.01	214	309	4.44	155	251	6.09	199	295	4.26	140	237	3.99
127	222	5.46	171	266	4.24	215	310	4.42	156	252	5.68	200	296	4.01	141	238	4.55
128	223	4.74	172	267	4.48	216	311	4.20	157	253	5.57	201	297	3.89	142	239	5.16
129	224	4.33	173	268	4.51	217	312	4.25	158	254	5.20	202	298	3.61	143	240	5.76
130	225	3.80	174	269	4.48	218	313	4.16	159	255	5.22	203	299	3.78	144	241	6.14
131	226	3.61	175	270	4.88	219	314	4.18	160	256	5.00	204	300	3.87	145	242	6.63
132	227	2.91	176	271	5.26	220	315	4.01	161	257	4.97	205	301	4.02	146	243	6.91
133	228	2.71	177	272	5.63	**$Z = 96$ (Cm)**			162	258	4.69	206	302	4.11	147	244	7.28
134	229	2.50	178	273	5.56	119	215	3.04	163	259	4.37	207	303	4.38	148	245	7.22

TABLE I. (*Continued*)

N	A	$B_{\rm f}$ (MeV)	N	A	$B_{\rm f}$ (MeV)	N	A	$B_{\rm f}$ (MeV)	N	A	$B_{\rm f}$ (MeV)	N	A	$B_{\rm f}$ (MeV)	N	A	$B_{\rm f}$ (MeV)
$Z = 97$ (Bk)			**$Z = 97$ (Bk)**			**$Z = 98$ (Cf)**			**$Z = 98$ (Cf)**			**$Z = 98$ (Cf)**			**$Z = 99$ (Es)**		
149	246	7.32	193	290	3.13	134	232	1.57	178	276	4.50	222	320	4.18	162	261	4.68
150	247	7.18	194	291	3.33	135	233	1.50	179	277	4.68	223	321	4.11	163	262	4.60
151	248	7.27	195	292	3.68	136	234	1.64	180	278	4.47	224	322	3.86	164	263	4.32
152	249	7.00	196	293	3.85	137	235	2.10	181	279	4.65	225	323	3.84	165	264	4.06
153	250	6.59	197	294	4.21	138	236	2.69	182	280	4.53	226	324	4.02	166	265	3.81
154	251	6.21	198	295	4.10	139	237	3.34	183	281	4.47	227	325	3.86	167	266	3.71
155	252	6.01	199	296	4.14	140	238	4.01	184	282	3.82	**$Z = 99$ (Es)**			168	267	3.60
156	253	5.59	200	297	3.98	141	239	4.64	185	283	2.86	125	224	2.29	169	268	3.51
157	254	5.50	201	298	4.05	142	240	5.22	186	284	2.00	126	225	2.51	170	269	3.50
158	255	5.10	202	299	3.99	143	241	5.83	187	285	1.50	127	226	1.80	171	270	3.82
159	256	5.09	203	300	4.17	144	242	6.16	188	286	1.27	128	227	0.98	172	271	3.85
160	257	4.80	204	301	4.20	145	243	6.55	189	287	1.51	129	228	1.01	173	272	4.08
161	258	4.58	205	302	4.42	146	244	6.69	190	288	1.70	130	229	0.70	174	273	3.96
162	259	4.51	206	303	4.43	147	245	6.99	191	289	2.00	131	230	1.30	175	274	4.06
163	260	4.42	207	304	4.59	148	246	7.16	192	290	2.21	132	231	1.30	176	275	3.82
164	261	4.21	208	305	4.66	149	247	7.35	193	291	2.52	133	232	1.44	177	276	4.17
165	262	4.03	209	306	4.95	150	248	7.24	194	292	2.69	134	233	1.46	178	277	4.10
166	263	3.80	210	307	4.90	151	249	7.31	195	293	3.05	135	234	1.56	179	278	4.27
167	264	3.80	211	308	4.99	152	250	7.09	196	294	3.21	136	235	1.83	180	279	4.02
168	265	3.72	212	309	4.84	153	251	6.64	197	295	3.59	137	236	2.38	181	280	4.12
169	266	3.74	213	310	4.82	154	252	6.07	198	296	3.73	138	237	2.96	182	281	3.95
170	267	3.70	214	311	4.70	155	253	5.62	199	297	3.94	139	238	3.59	183	282	3.99
171	268	4.07	215	312	4.61	156	254	5.27	200	298	3.85	140	239	4.32	184	283	3.39
172	269	4.09	216	313	4.44	157	255	5.21	201	299	4.04	141	240	4.95	185	284	2.60
173	270	4.32	217	314	4.53	158	256	4.82	202	300	4.10	142	241	5.32	186	285	1.75
174	271	4.19	218	315	4.45	159	257	4.56	203	301	4.27	143	242	5.70	187	286	1.46
175	272	4.33	219	316	4.45	160	258	4.43	204	302	4.28	144	243	5.98	188	287	1.21
176	273	4.49	220	317	4.28	161	259	4.57	205	303	4.43	145	244	6.28	189	288	1.40
177	274	4.77	221	318	4.31	162	260	4.64	206	304	4.48	146	245	6.53	190	289	1.63
178	275	4.69	222	319	4.08	163	261	4.54	207	305	4.63	147	246	6.90	191	290	1.80
179	276	4.93	223	320	4.06	164	262	4.30	208	306	4.64	148	247	7.07	192	291	2.06
180	277	4.71	224	321	3.78	165	263	4.06	209	307	4.86	149	248	7.44	193	292	2.39
181	278	4.86	**$Z = 98$ (Cf)**			166	264	3.81	210	308	4.81	150	249	7.38	194	293	2.57
182	279	4.70	123	221	3.09	167	265	3.77	211	309	4.91	151	250	7.48	195	294	2.77
183	280	4.61	124	222	3.39	168	266	3.68	212	310	4.76	152	251	7.24	196	295	3.00
184	281	3.87	125	223	3.89	169	267	3.64	213	311	4.83	153	252	6.79	197	296	3.22
185	282	2.95	126	224	4.04	170	268	3.65	214	312	4.56	154	253	6.22	198	297	3.42
186	283	2.17	127	225	3.41	171	269	3.98	215	313	4.62	155	254	5.67	199	298	3.76
187	284	2.09	128	226	2.65	172	270	4.09	216	314	4.47	156	255	5.05	200	299	3.95
188	285	2.00	129	227	1.99	173	271	4.27	217	315	4.56	157	256	5.01	201	300	4.21
189	286	2.29	130	228	1.39	174	272	4.18	218	316	4.50	158	257	4.50	202	301	4.26
190	287	2.43	131	229	1.58	175	273	4.11	219	317	4.49	159	258	4.32	203	302	4.42
191	288	2.70	132	230	1.58	176	274	4.30	220	318	4.30	160	259	4.43	204	303	4.42
192	289	2.84	133	231	1.67	177	275	4.56	221	319	4.30	161	260	4.64	205	304	4.53

TABLE I. (*Continued*)

N	A	B_f (MeV)	N	A	B_f (MeV)	N	A	B_f (MeV)	N	A	B_f (MeV)	N	A	B_f (MeV)	N	A	B_f (MeV)
$Z = 99$ (Es)			**$Z = 100$ (Fm)**			**$Z = 100$ (Fm)**			**$Z = 101$ (Md)**			**$Z = 101$ (Md)**			**$Z = 101$ (Md)**		
206	305	4.59	145	245	5.94	189	289	1.31	129	230	0.84	173	274	3.99	217	318	4.68
207	306	4.70	146	246	6.13	190	290	1.61	130	231	0.74	174	275	3.92	218	319	4.63
208	307	4.67	147	247	6.48	191	291	1.85	131	232	0.89	175	276	4.00	219	320	4.71
209	308	4.73	148	248	6.73	192	292	2.13	132	233	1.03	176	277	3.67	220	321	4.75
210	309	4.72	149	249	7.12	193	293	2.47	133	234	1.30	177	278	3.85	221	322	4.90
211	310	4.80	150	250	7.22	194	294	2.66	134	235	1.57	178	279	3.72	222	323	4.81
212	311	4.68	151	251	7.38	195	295	2.87	135	236	1.72	179	280	3.95	223	324	4.79
213	312	4.78	152	252	7.16	196	296	2.99	136	237	2.01	180	281	3.72	224	325	4.47
214	313	4.67	153	253	6.74	197	297	3.23	137	238	2.49	181	282	3.78	225	326	4.57
215	314	4.70	154	254	6.24	198	298	3.48	138	239	2.86	182	283	3.52	226	327	4.42
216	315	4.57	155	255	5.72	199	299	3.86	139	240	3.25	183	284	3.60	227	328	4.91
217	316	4.67	156	256	5.11	200	300	4.00	140	241	3.64	184	285	3.11	228	329	4.62
218	317	4.55	157	257	4.75	201	301	4.23	141	242	4.09	185	286	2.37	229	330	4.66
219	318	4.57	158	258	4.52	202	302	4.29	142	243	4.46	186	287	1.53	**$Z = 102$ (No)**		
220	319	4.39	159	259	4.54	203	303	4.44	143	244	4.80	187	288	1.26	130	232	0.83
221	320	4.56	160	260	4.62	204	304	4.34	144	245	5.11	188	289	1.15	131	233	0.75
222	321	4.39	161	261	4.68	205	305	4.41	145	246	5.47	189	290	1.38	132	234	0.97
223	322	4.25	162	262	4.82	206	306	4.46	146	247	5.74	190	291	1.71	133	235	1.03
224	323	4.01	163	263	4.75	207	307	4.52	147	248	6.03	191	292	1.99	134	236	1.27
225	324	4.01	164	264	4.49	208	308	4.41	148	249	6.24	192	293	2.28	135	237	1.59
226	325	3.83	165	265	4.23	209	309	4.50	149	250	6.70	193	294	2.63	136	238	2.05
227	326	4.13	166	266	3.94	210	310	4.50	150	251	6.98	194	295	2.69	137	239	2.35
228	327	3.74	167	267	3.74	211	311	4.60	151	252	7.23	195	296	2.95	138	240	2.55
229	328	3.91	168	268	3.60	212	312	4.52	152	253	7.01	196	297	3.13	139	241	2.82
$Z = 100$ (Fm)			169	269	3.58	213	313	4.66	153	254	6.61	197	298	3.49	140	242	3.18
126	226	2.84	170	270	3.58	214	314	4.54	154	255	6.13	198	299	3.74	141	243	3.58
127	227	2.08	171	271	3.87	215	315	4.63	155	256	5.69	199	300	3.97	142	244	3.94
128	228	0.80	172	272	3.91	216	316	4.50	156	257	5.09	200	301	4.13	143	245	4.32
129	229	0.90	173	273	4.14	217	317	4.63	157	258	4.84	201	302	4.36	144	246	4.62
130	230	0.79	174	274	4.06	218	318	4.55	158	259	4.67	202	303	4.31	145	247	4.98
131	231	0.85	175	275	4.12	219	319	4.57	159	260	4.92	203	304	4.46	146	248	5.24
132	232	1.25	176	276	3.77	220	320	4.58	160	261	4.99	204	305	4.38	147	249	5.61
133	233	1.39	177	277	4.13	221	321	4.76	161	262	5.05	205	306	4.39	148	250	5.83
134	234	1.46	178	278	4.06	222	322	4.51	162	263	5.12	206	307	4.41	149	251	6.25
135	235	1.56	179	279	4.25	223	323	4.53	163	264	4.89	207	308	4.39	150	252	6.50
136	236	1.87	180	280	4.03	224	324	4.20	164	265	4.59	208	309	4.29	151	253	6.93
137	237	2.39	181	281	4.13	225	325	4.27	165	266	4.31	209	310	4.32	152	254	6.76
138	238	2.88	182	282	3.93	226	326	4.11	166	267	3.99	210	311	4.36	153	255	6.38
139	239	3.49	183	283	3.96	227	327	4.51	167	268	3.75	211	312	4.50	154	256	5.94
140	240	4.14	184	284	3.43	228	328	4.25	168	269	3.57	212	313	4.46	155	257	5.52
141	241	4.50	185	285	2.58	229	329	4.32	169	270	3.54	213	314	4.59	156	258	4.98
142	242	4.88	186	286	1.71	230	330	3.98	170	271	3.47	214	315	4.54	157	259	5.00
143	243	5.29	187	287	1.29	**$Z = 101$ (Md)**			171	272	3.75	215	316	4.63	158	260	4.93
144	244	5.57	188	288	1.17	128	229	0.70	172	273	3.77	216	317	4.52	159	261	5.26

TABLE I. (*Continued*)

N	A	$B_{\rm f}$ (MeV)	N	A	$B_{\rm f}$ (MeV)	N	A	$B_{\rm f}$ (MeV)	N	A	$B_{\rm f}$ (MeV)	N	A	$B_{\rm f}$ (MeV)	N	A	$B_{\rm f}$ (MeV)
$Z = 102$ (No)			**$Z = 102$ (No)**			**$Z = 103$ (Lr)**			**$Z = 103$ (Lr)**			**$Z = 104$ (Rf)**			**$Z = 104$ (Rf)**		
160	262	5.11	204	306	4.23	150	253	6.27	194	297	2.68	143	247	3.33	187	291	1.37
161	263	5.26	205	307	4.24	151	254	6.70	195	298	2.93	144	248	3.64	188	292	1.11
162	264	5.36	206	308	4.13	152	255	6.60	196	299	3.24	145	249	3.95	189	293	1.24
163	265	5.40	207	309	4.12	153	256	6.27	197	300	3.59	146	250	4.36	190	294	1.27
164	266	5.01	208	310	4.11	154	257	5.90	198	301	3.74	147	251	4.76	191	295	1.61
165	267	4.72	209	311	4.12	155	258	5.52	199	302	4.01	148	252	5.09	192	296	1.94
166	268	4.19	210	312	4.15	156	259	5.21	200	303	4.08	149	253	5.53	193	297	2.24
167	269	3.96	211	313	4.30	157	260	5.39	201	304	4.27	150	254	5.87	194	298	2.55
168	270	3.74	212	314	4.27	158	261	5.37	202	305	4.22	151	255	6.24	195	299	2.70
169	271	3.69	213	315	4.39	159	262	5.52	203	306	4.39	152	256	6.26	196	300	3.12
170	272	3.66	214	316	4.38	160	263	5.48	204	307	4.36	153	257	6.02	197	301	3.42
171	273	3.93	215	317	4.49	161	264	5.73	205	308	4.23	154	258	5.65	198	302	3.57
172	274	3.95	216	318	4.44	162	265	5.97	206	309	4.14	155	259	5.49	199	303	3.80
173	275	4.22	217	319	4.58	163	266	6.03	207	310	4.03	156	260	5.36	200	304	3.90
174	276	4.11	218	320	4.56	164	267	5.63	208	311	3.99	157	261	5.56	201	305	4.09
175	277	4.22	219	321	4.64	165	268	5.22	209	312	4.07	158	262	5.59	202	306	4.11
176	278	3.86	220	322	4.78	166	269	4.81	210	313	4.06	159	263	5.61	203	307	4.34
177	279	3.93	221	323	5.08	167	270	4.36	211	314	4.20	160	264	5.79	204	308	4.18
178	280	3.84	222	324	4.99	168	271	3.96	212	315	4.21	161	265	6.27	205	309	4.11
179	281	4.07	223	325	4.98	169	272	3.78	213	316	4.34	162	266	6.43	206	310	4.01
180	282	3.80	224	326	4.82	170	273	3.69	214	317	4.38	163	267	6.43	207	311	3.93
181	283	4.02	225	327	5.06	171	274	3.94	215	318	4.56	164	268	6.03	208	312	3.86
182	284	3.72	226	328	5.00	172	275	3.94	216	319	4.53	165	269	5.60	209	313	3.89
183	285	3.80	227	329	5.50	173	276	4.21	217	320	4.68	166	270	5.10	210	314	3.88
184	286	3.21	228	330	5.07	174	277	4.13	218	321	4.63	167	271	4.72	211	315	4.01
185	287	2.41	**$Z = 103$ (Lr)**			175	278	4.23	219	322	4.77	168	272	4.28	212	316	4.03
186	288	1.61	132	235	1.07	176	279	3.87	220	323	4.90	169	273	4.06	213	317	4.24
187	289	1.29	133	236	1.18	177	280	3.76	221	324	5.28	170	274	3.82	214	318	4.31
188	290	0.98	134	237	1.44	178	281	3.65	222	325	5.18	171	275	4.06	215	319	4.50
189	291	1.20	135	238	1.75	179	282	3.91	223	326	5.28	172	276	4.10	216	320	4.46
190	292	1.62	136	239	1.95	180	283	3.62	224	327	5.18	173	277	4.43	217	321	4.61
191	293	1.89	137	240	2.12	181	284	3.86	225	328	5.41	174	278	4.37	218	322	4.56
192	294	2.19	138	241	2.28	182	285	3.58	226	329	5.31	175	279	4.45	219	323	4.93
193	295	2.54	139	242	2.46	183	286	3.61	227	330	6.00	176	280	4.10	220	324	5.09
194	296	2.62	140	243	2.79	184	287	2.99	**$Z = 104$ (Rf)**			177	281	4.17	221	325	5.41
195	297	2.95	141	244	3.18	185	288	2.26	134	238	1.11	178	282	4.12	222	326	5.40
196	298	3.17	142	245	3.49	186	289	1.61	135	239	1.28	179	283	4.43	223	327	5.58
197	299	3.54	143	246	3.89	187	290	1.32	136	240	1.53	180	284	4.22	224	328	5.55
198	300	3.66	144	247	4.19	188	291	1.04	137	241	1.67	181	285	4.19	225	329	5.76
199	301	3.86	145	248	4.50	189	292	1.22	138	242	1.82	182	286	3.95	226	330	5.68
200	302	4.06	146	249	4.81	190	293	1.51	139	243	2.01	183	287	3.96	**$Z = 105$ (Db)**		
201	303	4.30	147	250	5.26	191	294	1.89	140	244	2.28	184	288	3.23	136	241	1.31
202	304	4.19	148	251	5.55	192	295	2.19	141	245	2.54	185	289	2.38	137	242	1.44
203	305	4.42	149	252	5.97	193	296	2.51	142	246	2.95	186	290	1.80	138	243	1.55

TABLE I. (*Continued*)

N	A	$B_{\rm f}$ (MeV)	N	A	$B_{\rm f}$ (MeV)	N	A	$B_{\rm f}$ (MeV)	N	A	$B_{\rm f}$ (MeV)	N	A	$B_{\rm f}$ (MeV)	N	A	$B_{\rm f}$ (MeV)
$Z = 105$ (Db)			**$Z = 105$ (Db)**			**$Z = 106$ (Sg)**			**$Z = 106$ (Sg)**			**$Z = 107$ (Ns)**			**$Z = 107$ (Ns)**		
139	244	1.68	183	288	3.79	139	245	1.27	183	289	4.15	141	248	1.33	185	292	2.66
140	245	1.94	184	289	3.06	140	246	1.44	184	290	3.42	142	249	1.70	186	293	2.70
141	246	2.18	185	290	2.35	141	247	1.73	185	291	2.60	143	250	1.91	187	294	0.02
142	247	2.59	186	291	1.78	142	248	2.11	186	292	1.97	144	251	2.45	188	295	0.02
143	248	2.88	187	292	0.90	143	249	2.38	187	293	0.02	145	252	2.88	189	296	0.87
144	249	3.21	188	293	1.11	144	250	2.67	188	294	0.02	146	253	3.27	190	297	1.02
145	250	3.53	189	294	1.23	145	251	3.16	189	295	1.01	147	254	3.74	191	298	0.84
146	251	4.01	190	295	1.16	146	252	3.59	190	296	1.01	148	255	4.10	192	299	1.25
147	252	4.44	191	296	1.48	147	253	4.02	191	297	1.10	149	256	4.54	193	300	1.67
148	253	4.81	192	297	1.82	148	254	4.44	192	298	1.42	150	257	5.00	194	301	1.93
149	254	5.26	193	298	2.17	149	255	4.86	193	299	1.87	151	258	5.41	195	302	2.32
150	255	5.67	194	299	2.44	150	256	5.30	194	300	2.14	152	259	5.66	196	303	2.69
151	256	6.05	195	300	2.75	151	257	5.70	195	301	2.45	153	260	5.87	197	304	2.96
152	257	6.22	196	301	3.10	152	258	5.93	196	302	2.83	154	261	6.01	198	305	3.08
153	258	6.01	197	302	3.38	153	259	5.82	197	303	3.12	155	262	6.20	199	306	3.29
154	259	5.76	198	303	3.48	154	260	5.84	198	304	3.25	156	263	6.20	200	307	3.39
155	260	5.81	199	304	3.73	155	261	5.88	199	305	3.52	157	264	6.39	201	308	3.62
156	261	5.76	200	305	3.82	156	262	5.91	200	306	3.63	158	265	6.34	202	309	3.75
157	262	5.94	201	306	4.07	157	263	6.17	201	307	3.85	159	266	6.71	203	310	3.80
158	263	5.90	202	307	4.14	158	264	5.98	202	308	3.92	160	267	6.97	204	311	3.79
159	264	6.08	203	308	4.21	159	265	6.27	203	309	4.03	161	268	7.20	205	312	3.75
160	265	6.36	204	309	4.09	160	266	6.69	204	310	3.92	162	269	7.60	206	313	3.61
161	266	6.80	205	310	3.96	161	267	7.08	205	311	3.94	163	270	7.69	207	314	3.57
162	267	6.99	206	311	3.89	162	268	7.29	206	312	3.76	164	271	7.39	208	315	3.51
163	268	7.00	207	312	3.90	163	269	7.30	207	313	3.72	165	272	6.94	209	316	3.69
164	269	6.59	208	313	3.82	164	270	6.92	208	314	3.69	166	273	6.38	210	317	3.76
165	270	6.13	209	314	3.87	165	271	6.48	209	315	3.82	167	274	5.93	211	318	4.00
166	271	5.62	210	315	3.89	166	272	5.94	210	316	3.85	168	275	5.30	212	319	3.99
167	272	5.18	211	316	4.05	167	273	5.48	211	317	4.04	169	276	5.13	213	320	4.13
168	273	4.69	212	317	4.10	168	274	4.96	212	318	4.10	170	277	4.80	214	321	4.03
169	274	4.45	213	318	4.31	169	275	4.70	213	319	4.19	171	278	4.82	215	322	4.07
170	275	4.00	214	319	4.31	170	276	4.39	214	320	4.13	172	279	4.73	216	323	4.13
171	276	4.16	215	320	4.40	171	277	4.43	215	321	4.22	173	280	5.05	217	324	4.61
172	277	4.21	216	321	4.47	172	278	4.39	216	322	4.21	174	281	5.07	218	325	4.97
173	278	4.48	217	322	4.60	173	279	4.63	217	323	4.38	175	282	5.39	219	326	5.52
174	279	4.48	218	323	4.85	174	280	4.63	218	324	4.87	176	283	5.10	220	327	5.69
175	280	4.56	219	324	5.30	175	281	5.06	219	325	5.42	177	284	5.12	221	328	6.02
176	281	4.35	220	325	5.43	176	282	4.82	220	326	5.55	178	285	5.03	222	329	6.15
177	282	4.31	221	326	5.77	177	283	4.83	221	327	5.91	179	286	5.45	223	330	6.50
178	283	4.20	222	327	5.74	178	284	4.75	222	328	5.94	180	287	5.29	**$Z = 108$ (Hs)**		
179	284	4.59	223	328	5.99	179	285	5.05	223	329	6.19	181	288	5.36	142	250	1.02
180	285	4.37	224	329	5.92	180	286	4.91	224	330	6.13	182	289	4.93	143	251	1.55
181	286	4.40	225	330	6.18	181	287	4.91	**$Z = 107$ (Ns)**			183	290	4.74	144	252	1.97
182	287	3.86	**$Z = 106$ (Sg)**			182	288	4.44	140	247	1.13	184	291	4.15	145	253	2.39
			138	244	1.15												

TABLE I. (*Continued*)

N	A	$B_{\rm f}$ (MeV)	N	A	$B_{\rm f}$ (MeV)	N	A	$B_{\rm f}$ (MeV)	N	A	$B_{\rm f}$ (MeV)	N	A	$B_{\rm f}$ (MeV)	N	A	$B_{\rm f}$ (MeV)
$Z = 108$ (Hs)			**$Z = 108$ (Hs)**			**$Z = 109$ (Mt)**			**$Z = 109$ (Mt)**			**$Z = 110$ (Ds)**			**$Z = 110$ (Ds)**		
146	254	2.82	190	298	0.70	154	263	5.70	198	307	2.45	165	275	6.90	209	319	2.65
147	255	3.22	191	299	0.40	155	264	5.91	199	308	2.65	166	276	6.49	210	320	2.68
148	256	3.64	192	300	0.85	156	265	5.88	200	309	2.76	167	277	6.09	211	321	2.88
149	257	4.01	193	301	1.22	157	266	5.88	201	310	3.03	168	278	5.59	212	322	2.98
150	258	4.54	194	302	1.49	158	267	6.04	202	311	3.21	169	279	5.64	213	323	3.19
151	259	4.93	195	303	1.86	159	268	6.28	203	312	3.23	170	280	5.69	214	324	3.26
152	260	5.39	196	304	2.23	160	269	6.70	204	313	3.06	171	281	5.86	215	325	3.67
153	261	5.65	197	305	2.59	161	270	7.14	205	314	3.03	172	282	5.94	216	326	4.02
154	262	5.88	198	306	2.72	162	271	7.49	206	315	2.87	173	283	6.46	217	327	4.53
155	263	6.01	199	307	2.93	163	272	7.68	207	316	2.92	174	284	6.70	218	328	5.03
156	264	6.13	200	308	3.03	164	273	7.41	208	317	2.86	175	285	7.25	219	329	5.04
157	265	6.26	201	309	3.34	165	274	7.11	209	318	3.04	176	286	7.26	220	330	5.39
158	266	6.26	202	310	3.45	166	275	6.59	210	319	3.08	177	287	7.45	**$Z = 111$ (Rg)**		
159	267	6.47	203	311	3.47	167	276	6.16	211	320	3.33	178	288	7.45	148	259	2.32
160	268	6.59	204	312	3.43	168	277	5.63	212	321	3.35	179	289	7.61	149	260	2.71
161	269	7.04	205	313	3.38	169	278	5.44	213	322	3.48	180	290	7.33	150	261	3.20
162	270	7.37	206	314	3.22	170	279	5.31	214	323	3.50	181	291	7.21	151	262	3.62
163	271	7.49	207	315	3.23	171	280	5.47	215	324	3.72	182	292	6.73	152	263	4.21
164	272	7.30	208	316	3.18	172	281	5.48	216	325	4.14	183	293	6.46	153	264	4.42
165	273	6.93	209	317	3.32	173	282	5.79	217	326	4.62	184	294	5.85	154	265	4.75
166	274	6.45	210	318	3.41	174	283	5.88	218	327	4.99	185	295	4.91	155	266	4.72
167	275	6.08	211	319	3.65	175	284	6.30	219	328	5.44	186	296	4.39	156	267	4.80
168	276	5.52	212	320	3.64	176	285	6.22	220	329	5.48	187	297	3.51	157	268	4.88
169	277	5.68	213	321	3.78	177	286	6.51	221	330	5.83	188	298	2.75	158	269	5.10
170	278	5.50	214	322	3.69	178	287	6.51	**$Z = 110$ (Ds)**			189	299	2.07	159	270	5.70
171	279	5.18	215	323	3.82	179	288	6.96	146	256	1.76	190	300	0.59	160	271	6.13
172	280	5.27	216	324	3.93	180	289	6.56	147	257	2.12	191	301	0.22	161	272	6.62
173	281	5.62	217	325	4.58	181	290	6.51	148	258	2.68	192	302	0.24	162	273	6.96
174	282	5.51	218	326	4.92	182	291	6.10	149	259	3.15	193	303	0.23	163	274	7.20
175	283	5.76	219	327	5.44	183	292	5.86	150	260	3.70	194	304	0.61	164	275	7.01
176	284	5.74	220	328	5.57	184	293	5.26	151	261	4.17	195	305	1.04	165	276	6.71
177	285	6.01	221	329	5.92	185	294	4.38	152	262	4.68	196	306	1.36	166	277	6.37
178	286	5.89	222	330	6.11	186	295	3.78	153	263	4.99	197	307	1.75	167	278	6.06
179	287	6.43	**$Z = 109$ (Mt)**			187	296	3.06	154	264	5.27	198	308	2.04	168	279	5.70
180	288	6.25	144	253	1.59	188	297	2.24	155	265	5.35	199	309	2.21	169	280	6.01
181	289	6.24	145	254	1.96	189	298	1.12	156	266	5.34	200	310	2.46	170	281	6.03
182	290	5.83	146	255	2.37	190	299	0.06	157	267	5.47	201	311	2.83	171	282	6.37
183	291	5.59	147	256	2.76	191	300	0.13	158	268	5.48	202	312	2.88	172	283	6.64
184	292	5.02	148	257	3.22	192	301	0.07	159	269	5.95	203	313	2.87	173	284	7.26
185	293	4.02	149	258	3.58	193	302	0.83	160	270	6.45	204	314	2.76	174	285	7.55
186	294	3.31	150	259	4.20	194	303	1.15	161	271	6.92	205	315	2.72	175	286	8.06
187	295	2.62	151	260	4.65	195	304	1.57	162	272	7.31	206	316	2.55	176	287	7.87
188	296	0.01	152	261	5.13	196	305	1.90	163	273	7.48	207	317	2.56	177	288	7.90
189	297	0.83	153	262	5.48	197	306	2.23	164	274	7.27	208	318	2.46	178	289	7.98

TABLE I. (*Continued*)

N	A	$B_{\rm f}$ (MeV)	N	A	$B_{\rm f}$ (MeV)	N	A	$B_{\rm f}$ (MeV)	N	A	$B_{\rm f}$ (MeV)	N	A	$B_{\rm f}$ (MeV)	N	A	$B_{\rm f}$ (MeV)
$Z = 111$ (Rg)			**$Z = 112$ (Cn)**			**$Z = 112$ (Cn)**			**$Z = 113$ (X)**			**$Z = 113$ (X)**			**$Z = 114$ (Fl)**		
179	290	8.12	152	264	3.61	196	308	0.42	173	286	8.72	217	330	4.26	197	311	0.74
180	291	7.86	153	265	3.79	197	309	0.86	174	287	8.75	**$Z = 114$ (Fl)**			198	312	0.79
181	292	7.78	154	266	4.05	198	310	1.28	175	288	8.92	155	269	2.76	199	313	1.04
182	293	7.20	155	267	4.11	199	311	1.57	176	289	9.14	156	270	2.97	200	314	1.47
183	294	6.88	156	268	4.06	200	312	2.03	177	290	9.28	157	271	3.37	201	315	1.74
184	295	6.21	157	269	4.25	201	313	2.30	178	291	9.33	158	272	3.79	202	316	1.92
185	296	5.38	158	270	4.72	202	314	2.37	179	292	9.44	159	273	4.26	203	317	1.97
186	297	4.79	159	271	5.18	203	315	2.34	180	293	9.05	160	274	4.69	204	318	1.91
187	298	3.89	160	272	5.63	204	316	2.25	181	294	8.88	161	275	5.15	205	319	1.85
188	299	3.36	161	273	6.10	205	317	2.27	182	295	8.34	162	276	5.53	206	320	1.46
189	300	2.55	162	274	6.51	206	318	2.06	183	296	7.97	163	277	5.85	207	321	1.45
190	301	1.79	163	275	6.71	207	319	2.12	184	297	7.26	164	278	6.55	208	322	1.32
191	302	1.27	164	276	6.59	208	320	1.96	185	298	6.42	165	279	6.97	209	323	1.53
192	303	0.13	165	277	6.36	209	321	2.19	186	299	5.89	166	280	7.13	210	324	1.63
193	304	0.16	166	278	5.99	210	322	2.10	187	300	4.79	167	281	7.18	211	325	1.72
194	305	0.53	167	279	5.78	211	323	2.25	188	301	4.20	168	282	7.33	212	326	2.05
195	306	0.68	168	280	5.89	212	324	2.45	189	302	3.76	169	283	7.65	213	327	2.40
196	307	0.94	169	281	6.25	213	325	2.77	190	303	2.93	170	284	8.09	214	328	2.75
197	308	1.37	170	282	6.51	214	326	3.04	191	304	1.92	171	285	8.82	215	329	3.17
198	309	1.66	171	283	6.99	215	327	3.56	192	305	1.34	172	286	9.00	216	330	3.50
199	310	1.93	172	284	7.41	216	328	4.10	193	306	0.73	173	287	9.23	**$Z = 115$ (X)**		
200	311	2.21	173	285	8.00	217	329	4.54	194	307	0.50	174	288	9.18	157	272	3.08
201	312	2.58	174	286	8.24	218	330	4.76	195	308	0.31	175	289	9.61	158	273	3.47
202	313	2.64	175	287	8.40	**$Z = 113$ (X)**			196	309	0.37	176	290	9.89	159	274	3.86
203	314	2.59	176	288	8.53	153	266	3.06	197	310	0.79	177	291	9.97	160	275	4.29
204	315	2.51	177	289	8.59	154	267	3.25	198	311	0.85	178	292	9.98	161	276	4.75
205	316	2.52	178	290	8.74	155	268	3.25	199	312	1.26	179	293	9.89	162	277	5.20
206	317	2.29	179	291	8.82	156	269	3.38	200	313	1.70	180	294	9.53	163	278	5.61
207	318	2.34	180	292	8.58	157	270	3.80	201	314	2.00	181	295	9.35	164	279	6.51
208	319	2.21	181	293	8.44	158	271	4.26	202	315	2.11	182	296	8.87	165	280	6.70
209	320	2.45	182	294	7.96	159	272	4.77	203	316	2.22	183	297	8.47	166	281	6.82
210	321	2.38	183	295	7.60	160	273	5.22	204	317	2.09	184	298	7.82	167	282	7.18
211	322	2.54	184	296	6.93	161	274	5.70	205	318	2.13	185	299	6.92	168	283	7.60
212	323	2.60	185	297	6.03	162	275	6.09	206	319	1.91	186	300	6.43	169	284	8.18
213	324	2.90	186	298	5.52	163	276	6.38	207	320	1.95	187	301	5.25	170	285	8.58
214	325	3.27	187	299	4.37	164	277	6.31	208	321	1.80	188	302	4.68	171	286	8.96
215	326	3.81	188	300	4.32	165	278	6.06	209	322	1.96	189	303	3.50	172	287	9.20
216	327	4.24	189	301	3.09	166	279	6.12	210	323	1.86	190	304	3.68	173	288	9.42
217	328	4.73	190	302	2.30	167	280	6.41	211	324	2.02	191	305	2.36	174	289	9.29
218	329	4.95	191	303	1.54	168	281	6.66	212	325	2.24	192	306	1.83	175	290	9.53
219	330	5.15	192	304	0.96	169	282	6.98	213	326	2.60	193	307	0.94	176	291	9.60
$Z = 112$ (Cn)			193	305	0.55	170	283	7.35	214	327	2.88	194	308	0.71	177	292	9.76
150	262	2.65	194	306	0.05	171	284	7.93	215	328	3.43	195	309	0.53	178	293	9.87
151	263	3.15	195	307	0.09	172	285	8.33	216	329	3.91	196	310	0.57	179	294	9.93

TABLE I. (*Continued*)

N	A	$B_{\rm f}$ (MeV)	N	A	$B_{\rm f}$ (MeV)	N	A	$B_{\rm f}$ (MeV)	N	A	$B_{\rm f}$ (MeV)	N	A	$B_{\rm f}$ (MeV)	N	A	$B_{\rm f}$ (MeV)
$Z = 115$ (X)			**$Z = 116$ (Lv)**			**$Z = 116$ (Lv)**			**$Z = 117$ (X)**			**$Z = 118$ (X)**			**$Z = 119$ (X)**		
180	295	9.57	166	282	6.66	210	326	1.24	199	316	0.50	191	309	2.41	186	305	4.08
181	296	9.36	167	283	7.16	211	327	1.29	200	317	0.50	192	310	1.95	187	306	2.94
182	297	8.81	168	284	7.65	212	328	1.50	201	318	0.89	193	311	1.62	188	307	3.08
183	298	8.38	169	285	8.23	213	329	1.84	202	319	1.07	194	312	1.43	189	308	3.09
184	299	7.68	170	286	8.47	214	330	2.20	203	320	0.98	195	313	1.03	190	309	2.93
185	300	6.75	171	287	8.76	**$Z = 117$ (X)**			204	321	0.73	196	314	0.81	191	310	2.85
186	301	6.27	172	288	9.02	161	278	4.14	205	322	0.55	197	315	0.43	192	311	2.44
187	302	5.16	173	289	8.95	162	279	4.83	206	323	0.15	198	316	0.38	193	312	1.99
188	303	4.58	174	290	8.94	163	280	5.21	207	324	0.24	199	317	0.35	194	313	1.75
189	304	3.55	175	291	9.08	164	281	6.01	208	325	0.25	200	318	0.38	195	314	1.57
190	305	2.99	176	292	9.26	165	282	6.30	209	326	0.65	201	319	0.72	196	315	1.35
191	306	2.44	177	293	9.35	166	283	6.69	210	327	0.79	202	320	0.90	197	316	1.00
192	307	1.99	178	294	9.46	167	284	7.27	211	328	1.10	203	321	0.84	198	317	0.93
193	308	1.25	179	295	9.49	168	285	7.79	212	329	1.15	204	322	0.57	199	318	0.57
194	309	1.05	180	296	9.10	169	286	8.34	213	330	1.50	205	323	0.36	200	319	0.44
195	310	0.67	181	297	8.86	170	287	8.70	**$Z = 118$ (X)**			206	324	0.37	201	320	0.55
196	311	0.60	182	298	8.27	171	288	8.57	163	281	4.73	207	325	0.39	202	321	0.53
197	312	0.67	183	299	7.87	172	289	8.61	164	282	5.49	208	326	0.27	203	322	0.64
198	313	0.66	184	300	7.18	173	290	8.90	165	283	5.88	209	327	0.36	204	323	0.63
199	314	0.79	185	301	6.22	174	291	8.88	166	284	6.31	210	328	0.50	205	324	0.56
200	315	1.11	186	302	5.74	175	292	8.99	167	285	6.85	211	329	0.79	206	325	0.62
201	316	1.42	187	303	4.63	176	293	8.96	168	286	7.37	212	330	0.91	207	326	0.60
202	317	1.65	188	304	4.07	177	294	9.04	169	287	8.12	**$Z = 119$ (X)**			208	327	0.42
203	318	1.62	189	305	3.02	178	295	9.06	170	288	8.32	165	284	5.51	209	328	0.34
204	319	1.50	190	306	2.55	179	296	9.17	171	289	8.85	166	285	6.19	210	329	0.15
205	320	1.38	191	307	1.75	180	297	8.77	172	290	8.39	167	286	6.70	211	330	0.44
206	321	1.01	192	308	1.73	181	298	8.48	173	291	8.41	168	287	7.34	**$Z = 120$ (X)**		
207	322	0.81	193	309	0.93	182	299	7.87	174	292	8.41	169	288	7.90	167	287	6.35
208	323	0.85	194	310	0.72	183	300	7.42	175	293	8.53	170	289	8.06	168	288	6.85
209	324	1.24	195	311	0.44	184	301	6.78	176	294	8.48	171	290	7.62	169	289	7.35
210	325	1.51	196	312	0.41	185	302	5.83	177	295	8.46	172	291	7.80	170	290	7.70
211	326	1.58	197	313	0.63	186	303	5.35	178	296	8.36	173	292	8.05	171	291	8.26
212	327	1.76	198	314	0.61	187	304	4.24	179	297	8.49	174	293	8.13	172	292	7.36
213	328	2.10	199	315	0.61	188	305	3.66	180	298	8.05	175	294	8.29	173	293	7.44
214	329	2.50	200	316	0.90	189	306	2.66	181	299	7.76	176	295	8.06	174	294	7.57
215	330	3.08	201	317	1.28	190	307	2.26	182	300	7.15	177	296	8.07	175	295	7.71
$Z = 116$ (Lv)			202	318	1.47	191	308	2.04	183	301	6.67	178	297	7.94	176	296	7.69
159	275	3.32	203	319	1.36	192	309	1.77	184	302	6.01	179	298	8.10	177	297	7.54
160	276	3.79	204	320	1.16	193	310	1.35	185	303	5.08	180	299	7.72	178	298	7.33
161	277	4.25	205	321	1.09	194	311	1.07	186	304	4.54	181	300	7.37	179	299	7.48
162	278	4.91	206	322	0.63	195	312	0.48	187	305	3.38	182	301	6.71	180	300	7.01
163	279	5.35	207	323	0.53	196	313	0.24	188	306	2.90	183	302	6.22	181	301	6.68
164	280	6.21	208	324	0.63	197	314	0.43	189	307	2.61	184	303	5.54	182	302	6.07
165	281	6.41	209	325	0.97	198	315	0.49	190	308	2.49	185	304	4.64	183	303	5.55

TABLE I. (*Continued*)

N	A	$B_{\rm f}$ (MeV)	N	A	$B_{\rm f}$ (MeV)	N	A	$B_{\rm f}$ (MeV)	N	A	$B_{\rm f}$ (MeV)	N	A	$B_{\rm f}$ (MeV)	N	A	$B_{\rm f}$ (MeV)
$Z = 120$ (X)			**$Z = 121$ (X)**			**$Z = 122$ (X)**			**$Z = 123$ (X)**			**$Z = 125$ (X)**			**$Z = 126$ (X)**		
184	304	4.86	185	306	3.38	190	312	2.26	198	321	0.53	179	304	5.45	196	322	0.00
185	305	3.80	186	307	2.62	191	313	2.25	199	322	0.48	180	305	4.93	197	323	0.00
186	306	3.22	187	308	2.90	192	314	1.82	200	323	0.60	181	306	4.44	198	324	0.00
187	307	3.10	188	309	2.96	193	315	1.54	201	324	0.58	182	307	3.71	199	325	0.00
188	308	3.15	189	310	2.92	194	316	1.46	202	325	0.57	183	308	1.81	200	326	0.00
189	309	3.13	190	311	2.75	195	317	1.18	203	326	0.45	184	309	1.08	201	327	0.13
190	310	2.96	191	312	2.72	196	318	1.18	204	327	0.35	185	310	1.96	202	328	0.26
191	311	2.88	192	313	2.35	197	319	1.02	205	328	0.29	186	311	1.80	203	329	0.47
192	312	2.51	193	314	1.97	198	320	0.95	206	329	0.33	187	312	1.98	204	330	0.51
193	313	2.07	194	315	1.74	199	321	0.74	207	330	0.46	188	313	1.58	**$Z = 127$ (X)**		
194	314	1.84	195	316	1.51	200	322	0.77	**$Z = 124$ (X)**			189	314	1.82	183	310	2.63
195	315	1.69	196	317	1.45	201	323	0.74	176	300	5.64	190	315	1.74	184	311	2.08
196	316	1.58	197	318	1.36	202	324	0.66	177	301	5.77	191	316	1.58	185	312	2.15
197	317	1.31	198	319	1.25	203	325	0.48	178	302	5.63	192	317	1.11	186	313	1.93
198	318	1.19	199	320	1.04	204	326	0.46	179	303	5.45	193	318	0.79	187	314	2.02
199	319	0.92	200	321	0.89	205	327	0.35	180	304	4.12	194	319	0.45	188	315	2.07
200	320	0.81	201	322	0.90	206	328	0.38	181	305	3.90	195	320	0.08	189	316	2.26
201	321	0.80	202	323	0.89	207	329	0.49	182	306	3.32	196	321	0.00	190	317	2.05
202	322	0.81	203	324	0.71	208	330	0.41	183	307	2.74	197	322	0.00	191	318	1.56
203	323	0.79	204	325	0.62	**$Z = 123$ (X)**			184	308	2.01	198	323	0.00	192	319	1.11
204	324	0.68	205	326	0.50	174	297	6.09	185	309	1.85	199	324	0.00	193	320	1.00
205	325	0.54	206	327	0.57	175	298	5.84	186	310	1.75	200	325	0.19	194	321	0.47
206	326	0.58	207	328	0.63	176	299	5.60	187	311	1.74	201	326	0.35	195	322	0.12
207	327	0.55	208	329	0.17	177	300	5.54	188	312	1.66	202	327	0.32	196	323	0.00
208	328	0.49	209	330	0.70	178	301	5.45	189	313	1.45	203	328	0.40	197	324	0.00
209	329	0.52	**$Z = 122$ (X)**			179	302	5.45	190	314	1.35	204	329	0.33	198	325	0.00
210	330	0.40	172	294	6.32	180	303	5.01	191	315	1.27	205	330	0.31	199	326	0.00
$Z = 121$ (X)			173	295	6.54	181	304	4.93	192	316	1.10	**$Z = 126$ (X)**			200	327	0.00
169	290	7.07	174	296	6.53	182	305	4.25	193	317	0.96	180	306	4.69	201	328	0.00
170	291	6.46	175	297	6.31	183	306	3.69	194	318	0.78	181	307	4.09	202	329	0.11
171	292	6.82	176	298	6.33	184	307	2.95	195	319	0.39	182	308	3.51	203	330	0.39
172	293	6.89	177	299	6.28	185	308	1.94	196	320	0.13	183	309	2.60	**$Z = 128$ (X)**		
173	294	7.31	178	300	6.19	186	309	1.14	197	321	0.00	184	310	1.80	185	313	2.00
174	295	7.03	179	301	6.23	187	310	2.10	198	322	0.00	185	311	2.08	186	314	1.71
175	296	7.19	180	302	5.60	188	311	2.01	199	323	0.21	186	312	1.87	187	315	2.10
176	297	7.16	181	303	5.51	189	312	1.90	200	324	0.34	187	313	1.85	188	316	2.11
177	298	7.05	182	304	4.87	190	313	1.81	201	325	0.47	188	314	1.75	189	317	2.15
178	299	6.99	183	305	4.33	191	314	1.81	202	326	0.43	189	315	2.01	190	318	1.93
179	300	7.10	184	306	3.62	192	315	1.38	203	327	0.48	190	316	1.84	191	319	1.57
180	301	6.66	185	307	2.60	193	316	1.36	204	328	0.37	191	317	1.67	192	320	1.26
181	302	6.31	186	308	1.82	194	317	1.31	205	329	0.36	192	318	1.17	193	321	0.93
182	303	5.64	187	309	2.45	195	318	1.01	206	330	0.16	193	319	0.91	194	322	0.67
183	304	5.11	188	310	2.41	196	319	0.82	**$Z = 125$ (X)**			194	320	0.36	195	323	0.36
184	305	4.40	189	311	2.38	197	320	0.63	178	303	5.64	195	321	0.00	196	324	0.12

TABLE I. (*Continued*)

N	A	$B_{\rm f}$ (MeV)	N	A	$B_{\rm f}$ (MeV)	N	A	$B_{\rm f}$ (MeV)	N	A	$B_{\rm f}$ (MeV)	N	A	$B_{\rm f}$ (MeV)	N	A	$B_{\rm f}$ (MeV)
$Z = 128$ (X)																	
197	325	0.00															
198	326	0.00															
199	327	0.00															
200	328	0.00															
201	329	0.00															
202	330	0.18															
$Z = 129$ (X)																	
187	316	2.05															
188	317	2.01															
189	318	1.93															
190	319	1.81															
191	320	1.59															
192	321	1.31															
193	322	1.12															
194	323	0.90															
195	324	0.50															
196	325	0.24															
197	326	0.00															
198	327	0.00															
199	328	0.00															
200	329	0.00															
201	330	0.00															
$Z = 130$ (X)																	
189	319	2.03															
190	320	1.91															
191	321	1.69															
192	322	1.22															
193	323	1.18															
194	324	0.85															
195	325	0.45															
196	326	0.20															
197	327	0.03															
198	328	0.00															
199	329	0.00															
200	330	0.00															